Article

In vivo monoclonal antibody efficacy against SARS-CoV-2 variant strains

https://doi.org/10.1038/s41586-021-03720-y

Received: 21 April 2021

Accepted: 11 June 2021

Published online: 21 June 2021

Check for updates

Rita E. Chen[1,2,20], Emma S. Winkler[1,2,20], James Brett Case[1,20], Ishmael D. Aziati[1], Traci L. Bricker[1], Astha Joshi[1], Tamarand L. Darling[1], Baoling Ying[1], John M. Errico[2], Swathi Shrihari[1], Laura A. VanBlargan[1], Xuping Xie[3], Pavlo Gilchuk[4], Seth J. Zost[4], Lindsay Droit[5], Zhuoming Liu[5], Spencer Stumpf[5], David Wang[5], Scott A. Handley[2], W. Blaine Stine Jr[6], Pei-Yong Shi[3,7,8], Meredith E. Davis-Gardner[9], Mehul S. Suthar[9], Miguel Garcia Knight[10], Raul Andino[10], Charles Y. Chiu[11,12], Ali H. Ellebedy[2,13,14], Daved H. Fremont[2,5,15], Sean P. J. Whelan[5], James E. Crowe Jr[4,16,17], Lisa Purcell[18], Davide Corti[19], Adrianus C. M. Boon[1,2,5] & Michael S. Diamond[1,2,5,13,14] ✉

Rapidly emerging SARS-CoV-2 variants jeopardize antibody-based countermeasures. Although cell culture experiments have demonstrated a loss of potency of several anti-spike neutralizing antibodies against variant strains of SARS-CoV-2[1–3], the in vivo importance of these results remains uncertain. Here we report the in vitro and in vivo activity of a panel of monoclonal antibodies (mAbs), which correspond to many in advanced clinical development by Vir Biotechnology, AbbVie, AstraZeneca, Regeneron and Lilly, against SARS-CoV-2 variant viruses. Although some individual mAbs showed reduced or abrogated neutralizing activity in cell culture against B.1.351, B.1.1.28, B.1.617.1 and B.1.526 viruses with mutations at residue E484 of the spike protein, low prophylactic doses of mAb combinations protected against infection by many variants in K18-hACE2 transgenic mice, 129S2 immunocompetent mice and hamsters, without the emergence of resistance. Exceptions were LY-CoV555 monotherapy and LY-CoV555 and LY-CoV016 combination therapy, both of which lost all protective activity, and the combination of AbbVie 2B04 and 47D11, which showed a partial loss of activity. When administered after infection, higher doses of several mAb cocktails protected in vivo against viruses with a B.1.351 spike gene. Therefore, many—but not all—of the antibody products with Emergency Use Authorization should retain substantial efficacy against the prevailing variant strains of SARS-CoV-2.

Variant strains of SARS-CoV-2 have been detected in the UK (B.1.1.7, also known as Alpha), South Africa (B.1.351, also known as Beta), Brazil (B.1.1.28 (also known as P.1, also known as Gamma)) and elsewhere that contain substitutions in the N-terminal domain and the receptor-binding motif of the receptor-binding domain (RBD). Cell-based assays suggest that neutralization by many antibodies may be diminished against variants that express spike mutations, especially at position E484[1–5]. However, the in vivo implications of this loss of mAb neutralizing activity remains uncertain, particularly forcombination mAb therapies.

To evaluate the effects of SARS-CoV-2 strain variation on mAb protection, we assembled a panel of infectious SARS-CoV-2 strains with sequence substitutions in the spike gene (Fig. 1a, b) including a B.1.1.7 isolate from the UK, a B.1.429 isolate from California (USA), a B.1.617.1 isolate (of a clade identified in India) and two B.1.526 isolates from New York (USA). We also used SARS-CoV-2 strains from Washington (USA) with a D614G substitution (WA1/2020 D614G) or with both N501Y and D614G substitutions (WA1/2020 N501Y/D614G) as well as chimeric SARS-CoV-2 strains with B.1.351 or B.1.1.28 spike genes in the Washington strain background (denoted Wash-B.1.351 and Wash-B.1.1.28, respectively)[1,6]. All viruses were propagated in Vero cells expressing transmembrane protease serine 2 (Vero-TMPRSS2 cells) to prevent the emergence of mutations at or near the furin cleavage site in the spike protein that affect virulence[7]. All viruses were deep-sequenced

[1]Department of Medicine, Washington University School of Medicine, St Louis, MO, USA. [2]Department of Pathology and Immunology, Washington University School of Medicine, St Louis, MO, USA. [3]Department of Biochemistry and Molecular Biology, University of Texas Medical Branch, Galveston, TX, USA. [4]Vanderbilt Vaccine Center, Vanderbilt University Medical Center, Nashville, TN, USA. [5]Department of Molecular Microbiology, Washington University School of Medicine, St Louis, MO, USA. [6]AbbVie Bioresearch Center, Worcester, MA, USA. [7]Department of Microbiology and Immunology, University of Texas Medical Branch, Galveston, TX, USA. [8]Sealy Institute for Vaccine Sciences, University of Texas Medical Branch, Galveston, TX, USA. [9]Center for Childhood Infections and Vaccines of Children's Healthcare of Atlanta, Department of Pediatrics, Emory Vaccine Center, Emory University School of Medicine, Atlanta, GA, USA. [10]Department of Microbiology and Immunology, University of California San Francisco, San Francisco, CA, USA. [11]Department of Laboratory Medicine, University of California San Francisco, San Francisco, CA, USA. [12]Department of Medicine, University of California San Francisco, San Francisco, CA, USA. [13]Andrew M. and Jane M. Bursky Center for Human Immunology and Immunotherapy Programs, Washington University School of Medicine, St Louis, MO, USA. [14]Center for Vaccines and Immunity to Microbial Pathogens, Washington University School of Medicine, St Louis, MO, USA. [15]Department of Biochemistry and Molecular Biophysics, Washington University School of Medicine, St Louis, MO, USA. [16]Department of Pediatrics, Vanderbilt University Medical Center, Nashville, TN, USA. [17]Department of Pathology, Microbiology and Immunology, Vanderbilt University Medical Center, Nashville, TN, USA. [18]Vir Biotechnology, St Louis, MO, USA. [19]Humabs BioMed SA, a subsidiary of Vir Biotechnology, Bellinzona, Switzerland. [20]These authors contributed equally: Rita E. Chen, Emma S. Winkler, James Brett Case. ✉e-mail: diamond@wusm.wustl.edu

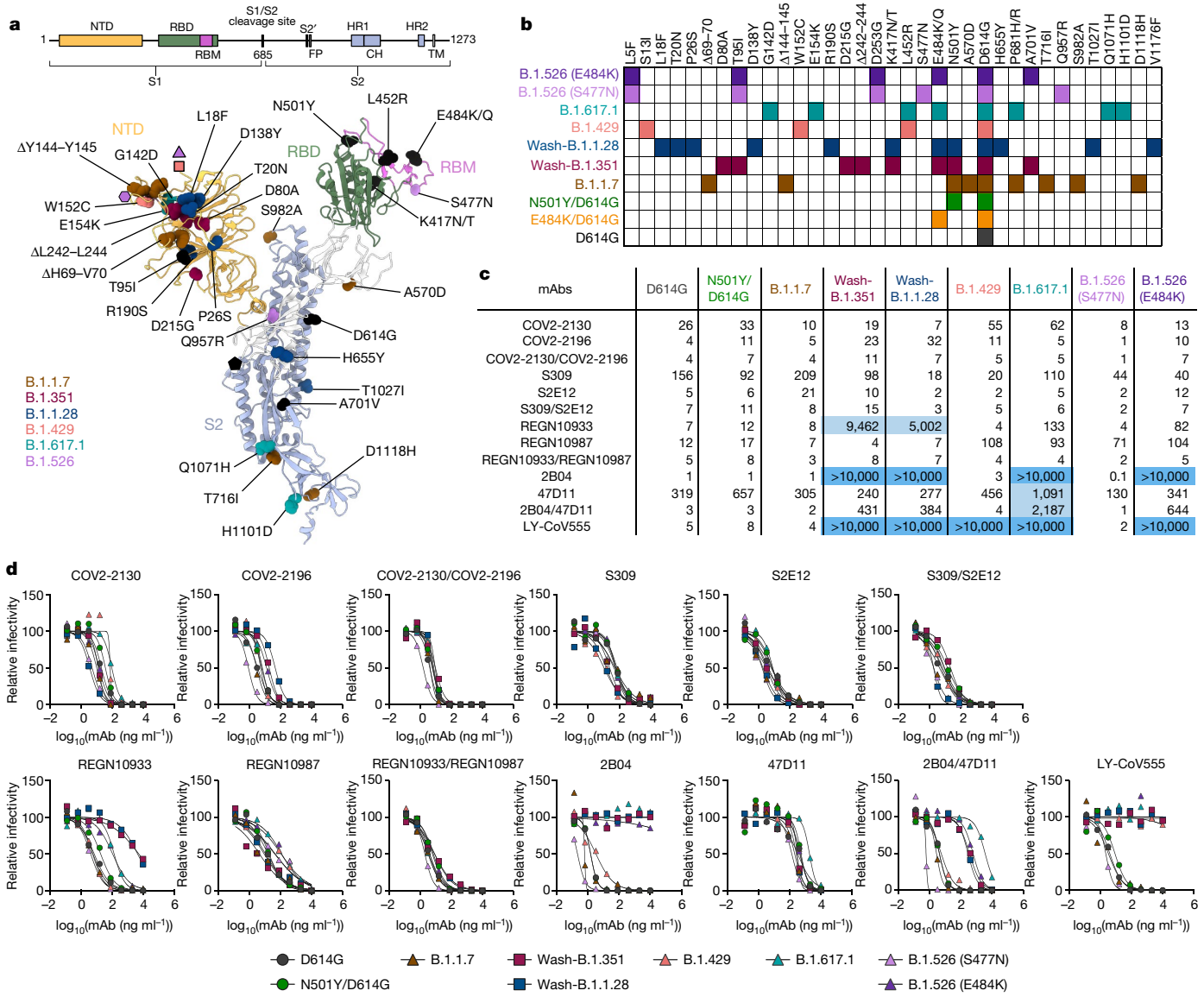

Fig. 1 | Neutralization of SARS-CoV-2 variant strains by clinically relevant mAbs. a, **b**, Amino acid substitutions in SARS-CoV-2 variants mapped onto the structure of the spike protein. Schematic layout of the spike protein monomer is depicted at the top. Structure of spike monomer (Protein Data Bank code (PDB) 7C2L, with RBD from PDB 6W41) is depicted as a cartoon, with the N-terminal domain (NTD), RBD, receptor-binding motif (RBM) and S2 coloured in orange, green, magenta and light blue, respectively. Substitutions for each variant are shown as spheres and coloured according to the legend. Substitutions shown in black are shared between several variants. The purple triangle, pink square, purple hexagon and black pentagon represent approximate locations of L5, S13, D253 and P681, respectively, which were not modelled in the original structures. CH, central helix; FP, fusion peptide; HR, heptad repeat; TM, transmembrane domain. The structural figure in **a** was generated using UCSF ChimeraX[33]. **b**, Viruses used with indicated coloured mutations in the spike protein. **c**, Summary of EC_{50} values (ng ml^{-1}) of neutralization of SARS-CoV-2 viruses performed in Vero-TMPRSS2 cells. Blue shading of cells indicates a partial (EC_{50} > 1,000 ng ml^{-1}) or complete (EC_{50} > 10,000 ng ml^{-1}) loss of neutralizing activity. **d**, Neutralization curves comparing the sensitivity of SARS-CoV-2 strains to the indicated individual or combinations of mAbs. Data are representative of two to five experiments, each performed in technical duplicate.

to confirm the presence of expected mutations before use (Supplementary Table 1).

We first assessed the effect of SARS-CoV-2 spike variation on antibody neutralization (Fig. 1c, d). We tested individual mAbs and cocktails of mAbs in clinical development that target the RBD, including 2B04 and 47D11 (AbbVie), S309 and S2E12 (Vir Biotechnology), COV2-2130 and COV2-2196 (Vanderbilt University Medical Center, with derivatives being evaluated by AstraZeneca), REGN10933 and REGN10987 (synthesized on the basis of casirivimab and imdevimab sequences from Regeneron), and LY-CoV555 (synthesized on the basis of bamlanivimab sequences from Lilly). All individual mAbs tested efficiently neutralized the WA1/2020 D614G, WA1/2020 N501Y/D614G and B.1.1.7 strains, and several mAbs (COV2-2130, COV2-2196, S309, S2E12 and 47D11) showed little change in potency against the Wash-B.1.351, Wash-B.1.1.28, B.1.429 and B.1.526 strains (Fig. 1c, d). By comparison, REGN10987 and LY-CoV555 showed an approximately 10-fold and complete loss, respectively, in inhibitory activity against the B.1.429 and B.1.617.1 strains, which is consistent with previous studies that have identified L452 and adjacent residues as interaction sites for these mAbs[8] (Supplementary Table 2). Moreover, REGN10933, LY-CoV555 and 2B04 exhibited a substantial or complete loss of neutralizing activity against Wash-B.1.351, Wash-B.1.1.28, B.1.617.1 and B.1.526 (E484K) viruses that contain mutations at residue E484 (Fig. 1c, d, Extended Data Fig. 1), which corresponds with structural and mapping studies

(Supplementary Table 2). Analysis of mAb cocktails showed that COV2-2130 in combination with COV2-2196 (COV2-2130/COV2-2196), S309/S2E12 and REGN10933/REGN10987 neutralized all of the virus strains we tested; the last of these combinations retained potency corresponding to the mAb with inhibitory activity in the cocktail for a given virus. The 2B04/47D11 mAb combination efficiently neutralized WA1/2020 D614G, WA1/2020 N501Y/D614G, B.1.1.7 and B.1.429 strains, whereas the activity of this combination against Wash-B.1.351, Wash-B.1.1.28, B.1.617.1 and B.1.526 (E484K) reflected the less-potent 47D11 mAb component (half-maximal effective concentration (EC_{50}) of 384–2,187 ng ml^{-1}) (Fig. 1c, d). Additional mutations in B.1.617.1 decreased the potency of the 2B04/47D11 combination further. By contrast, almost all of the mAbs retained neutralizing potency against B.1.526 (S477N).

Prophylactic efficacy against variants

To evaluate the efficacy of the mAb combinations in vivo, we initially used K18-hACE2 mice in which human ACE2 expression is driven by the cytokeratin 18 gene promoter[9,10]. In previous studies it was established that low (2 mg per kg body weight (mg kg^{-1})) doses of several anti-RBD neutralizing human mAbs provide a threshold of protection when administered as prophylaxis[11]. Accordingly, we gave K18-hACE2 mice a single 40-μg (about 2 mg kg^{-1} total) dose of the mAb combinations (2B04/47D11, S309/S2E12, COV2-2130/COV2-2196 or REGN10933/REGN10987) or LY-CoV555 as monotherapy by intraperitoneal injection one day before intranasal inoculation with SARS-CoV-2 (WA1/2020 N501Y/D614G, B.1.1.7, Wash-B.1.351 or Wash-B.1.1.28). For these in vivo studies, we used a recombinant version of WA1/2020 that encodes N501Y for direct comparison to B.1.1.7, Wash-B.1.351 or Wash-B.1.1.28 (all of which contain this residue). This substitution increases infection in mice[12,13], but did not substantively affect neutralization of the mAbs we tested (Fig. 1c).

Compared to a control human mAb, a single 40-μg prophylaxis dose of the anti-SARS-CoV-2 mAbs conferred substantial protection against WA1/2020-N501Y/D614G-induced weight loss and viral burden in the lungs, nasal washes, brain, spleen and heart in the K18-hACE2 mice at 6 days after infection (Fig. 2a–c, Extended Data Figs. 2, 3a). Although all of the anti-SARS-CoV-2 mAb cocktails protected against weight loss caused by B.1.1.7 (Fig. 2d), Wash-B.1.351 (Fig. 2g) or Wash-B.1.1.28 (Fig. 2j), LY-CoV555 monotherapy protected only against the B.1.1.7 strain (Fig. 2d, g, j). Some of the antibodies provided less virological protection against the B.1.1.7 (Fig. 2e, f), Wash-B.1.351 (Fig. 2h, i) or Wash-B.1.1.28 (Fig. 2k, l) strains in specific tissues. Whereas all mAb groups protected against B.1.1.7 infection in the lung (Fig. 2e), 2B04/47D11 or LY-CoV555 did not perform as well in nasal washes (Fig. 2f), and LY-CoV555 showed reduced protection in the brain (Extended Data Fig. 2). Sanger sequencing analysis of the RBD region of viral RNA of brain, nasal wash and lung samples from mice treated with these mAbs did not show evidence of neutralization escape (Supplementary Table 3). Mice treated with 2B04/47D11 or LY-CoV555 also showed greater virus breakthrough than those treated with the other tested antibodies when challenged with Wash-B.1.351 (Fig. 2h, i) or Wash-B.1.1.28 (Fig. 2k, l) viruses: 2B04/47D11 reduced viral burden in the lungs, nasal washes and brain much less efficiently than the other mAb cocktails, and LY-CoV555 mAb treatment conferred virtually no protection in any tissue analysed (Fig. 2h, i, k, l, Extended Data Figs. 2, 3b). Compared to COV2-2130/COV2-2196 and S309/S2E12, REGN10933/REGN10987 also showed less ability to reduce viral RNA levels in nasal washes of mice infected with Wash-B.1.351 (Fig. 2i) or Wash-B.1.1.28 (Fig. 2l) viruses. To confirm that our findings with Wash-B.1.351 are similar to a bona fide B.1.351 strain, we tested mAbs from each cocktail for neutralization and the COV2-2130/COV2-2196 cocktail for protection in K18-hACE2 mice. Equivalent levels of neutralization and viral burden reduction were seen with B.1.351 and Wash-B.1.351 viruses (Extended Data Fig. 4).

To evaluate further the extent of protection conferred by the different mAb groups against the SARS-CoV-2 variant viruses, we measured pro-inflammatory cytokine and chemokines in lung homogenates collected at six days after infection (Extended Data Figs. 5, 6). This analysis showed a strong correspondence with viral RNA levels in the lung: (1) compared to the control mAb, S309/S2E12, COV2-2130/COV2-2196 and REGN10933/REGN10987 combinations showed markedly reduced levels of pro-inflammatory cytokines and chemokines (G-CSF, IFNγ, IL-6, CXCL10, LIF, CCL2, CXCL9, CCL3 and CCL4) after infection with WA1/2020 N501Y/D614G, B.1.1.7, Wash-B.1.351 or Wash-B.1.1.28; and (2) prophylaxis with 2B04/47D11 or LY-CoV555 resulted in reduced inflammatory cytokine and chemokine levels in mice infected with WA1/2020 N501Y/D614G and B.1.1.7, with less improvement in mice infected with Wash-B.1.351 or Wash-B.1.1.28.

Given that a 40-μg dose of the S309/S2E12, COV2-2130/COV2-2196 and REGN10933/REGN10987 combinations prevented infection and inflammation caused by the different SARS-CoV-2 strains, we tested a tenfold-lower (4 μg) dose (about 0.2 mg kg^{-1}) to assess for possible differences in protection. Prophylaxis with COV2-2130/COV2-2196, S309/S2E12, REGN10933/REGN10987 or 2B04/47D11 protected K18-hACE2 mice against weight loss caused by all four viruses (Extended Data Fig. 7a–d). Whereas the COV2-2130/COV2-2196, S309/S2E12 and REGN10933/REGN10987 mAb combinations reduced viral RNA levels in the lung at six days after infection in K18-hACE2 mice infected with WA1/2020 N501Y/D614G, B.1.1.7, Wash-B.1.351 or Wash-B.1.1.28, the 2B04/47D11 treatment conferred protection against B.1.1.7 and WA1/2020 N501Y/D614G but not against Wash-B.1.351 or Wash-B.1.1.28 viruses at this lower dose (Extended Data Fig. 7e–h). By comparison, in nasal washes, all four mAb cocktails resulted in relatively similar reductions in viral RNA levels at six days after infection of mice inoculated with WA1/2020 N501Y/D614G, B.1.1.7, Wash-B.1.351 or Wash-B.1.1.28 (Extended Data Fig. 7i–l). Even at this low treatment dose, with the exception of some breakthrough events (>6 $\log_{10}$(copies of *N* per mg): COV2-2130/COV2-2196 (2 of 24 mice); S309/S2E12 (6 of 24 mice); REGN10933/REGN10987 (1 of 24 mice); and 2B04/47D11 (6 of 24 mice)), the mAb combinations generally prevented infection of the brain (Extended Data Fig. 7m–p, Supplementary Table 3). Overall, the neutralization activity of mAbs in vitro against SARS-CoV-2 variants correlated with lung viral burden after prophylactic administration (Extended Data Fig. 8).

As an alternative model for evaluating mAb efficacy, we tested immunocompetent, inbred 129S2 mice, which are permissive to infection by SARS-CoV-2 strains that encode an N501Y substitution without human ACE2 expression[12,13]; presumably, the N501Y adaptive mutation enables engagement of mouse ACE2. We administered a single 40-μg (about 2 mg kg^{-1}) dose of mAb cocktails (COV2-2130/COV2-2196, S309/S2E12 or REGN10933/REGN10987) or a control mAb via intraperitoneal injection one day before intranasal inoculation with 10^3 focus-forming units (FFU) of WA1/2020 N501Y/D614G, Wash-B.1.351 or Wash-B.1.1.28, and 10^5 FFU of B.1.1.7 (Extended Data Fig. 9). A higher inoculating dose of B.1.1.7 was required to obtain equivalent levels of viral RNA in the lung compared to the other three viruses. At three days after infection, we collected tissues for viral burden analyses; at this time point, reproducible weight loss was not observed. All three mAb cocktails tested (COV2-2130/COV2-2196, S309/S2E12 and REGN10933/REGN10987) protected 129S2 mice against infection in the lung by all of the SARS-CoV-2 strains (Extended Data Fig. 9a–d); despite some variability, we observed a trend towards less complete protection in mice infected with Wash-B.1.351 and Wash-B.1.1.28 strains (Extended Data Fig. 3c–f). When we evaluated the nasal washes, reductions in viral RNA levels were diminished with the Wash-B.1.351 virus, especially for the COV2-2130/COV2-2196 and REGN10933/REGN10987 combinations (Extended Data Fig. 9e–h). Sequencing analysis of lung samples from the infected 129S2 mice also did not reveal evidence of acquisition of mutations in the RBD (Supplementary Table 3).

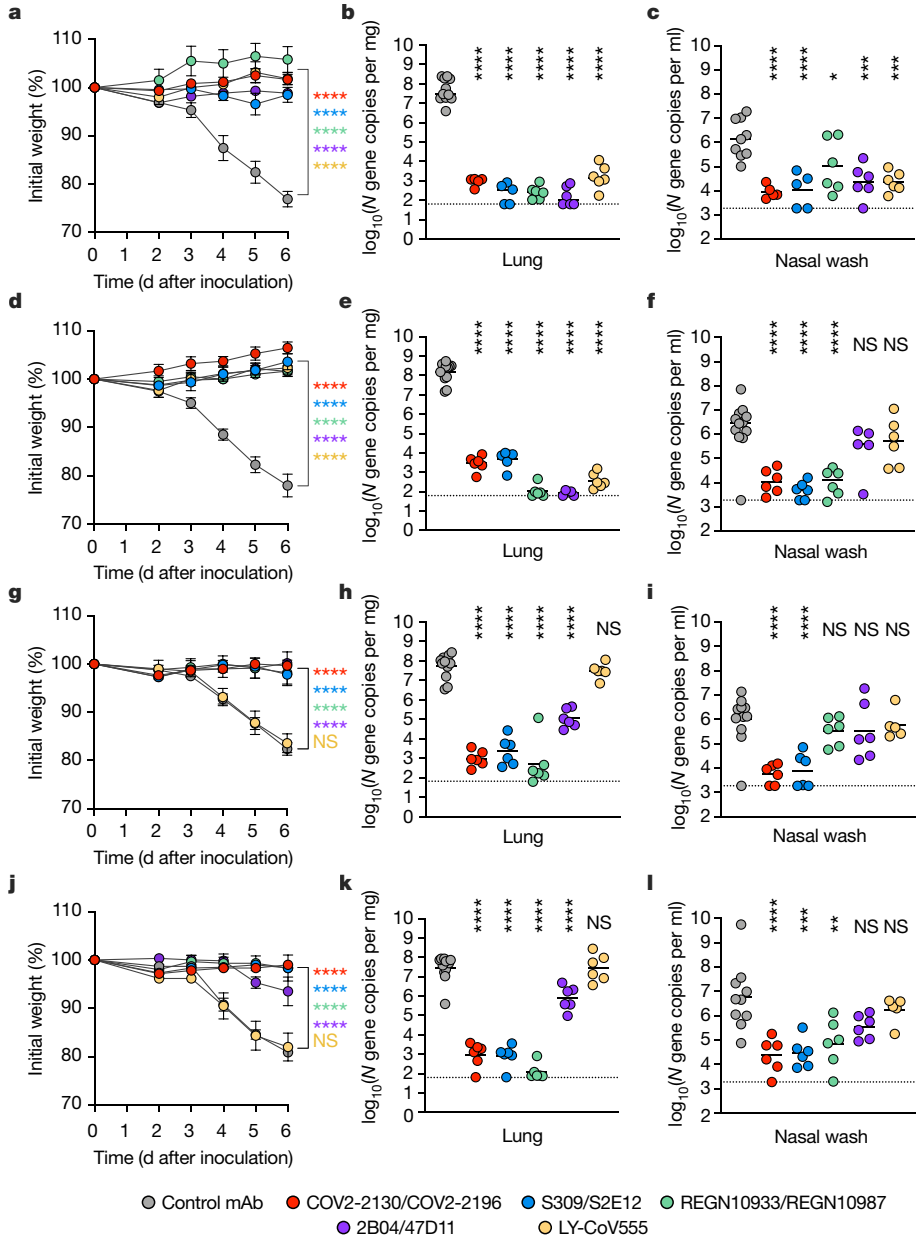

Fig. 2 | Antibody prophylaxis against SARS-CoV-2 variants in K18-hACE2 mice. a–**l**, Eight-to-ten-week-old female and male K18-hACE2 transgenic mice received 40 μg (about 2 mg kg^{-1}) of the indicated mAb treatment by intraperitoneal injection one day before intranasal inoculation with 10^3 FFU of the SARS-CoV-2 N501Y/D614G (**a**–**c**), B.1.1.7 (**d**–**f**), Wash-B.1.351 (**g**–**i**) or Wash-B.1.1.28 (**j**–**l**) strains. Tissues were collected at six days after infection. **a**, **d**, **g**, **j**, Weight change after infection with SARS-CoV-2 (mean ± s.e.m.; $n = 6$–12 mice per group, two experiments; one-way analysis of variance (ANOVA) with Dunnett's test of area under the curve. NS, not significant; ****$P < 0.0001$). Viral RNA levels in the lung (**b**, **e**, **h**, **k**) and nasal washes (**c**, **f**, **i**, **l**) were measured (line indicates median; in order from left to right, $n = 9, 6, 7, 6, 6$ and 6 (**a**); $n = 11, 5, 5, 6, 6$ and 6 (**b**); $n = 9, 5, 5, 6, 6$ and 6 (**c**); $n = 12, 6, 6, 6, 5$ and 6 (**d**–**f**); $n = 12, 6, 6, 6, 6$ and 6 (**g**, **h**, **j**, **k**); $n = 12, 6, 6, 6, 6$ and 5 (**i**); $n = 10, 6, 6, 6, 6$ and 5 (**l**) mice per group, two experiments; one-way ANOVA with Dunnett's test with comparison to control mAb. NS, not significant, ****$P < 0.0001$; *$P = 0.026$ (**c**); **$P = 0.0016$, ***$P = 0.0002$ (**l**)). Dotted line indicates the limit of detection of the assay.

The immunocompetent Syrian golden hamster has previously been used to evaluate mAb activity against SARS-CoV-2 infection[14,15]. We used this model to assess independently the inhibitory activity and possible emergence of resistance of one of the mAb combinations (COV2-2130/COV2-2196) against viruses containing the B.1.351 spike protein. One day before intranasal inoculation with 5×10^5 FFU of Wash-B.1.351 or WA1/2020 D614G, we treated hamsters with a single 800-μg (about 10 mg kg^{-1}) or 320-μg (about 4 mg kg^{-1}) dose of the COV2-2130/COV2-2196 cocktail or isotype control mAb by intraperitoneal injection (Extended Data Fig. 10). Weights were followed for four days, and tissues were collected for virological and cytokine analysis. At the 800-μg mAb cocktail dose, hamsters treated with COV2-2130/COV2-2196 and infected with WA1/2020 D614G or Wash-B.1.351 showed protection against weight loss and reduced viral burden levels in the lungs, but not nasal swabs, compared to the isotype control mAb (Extended Data Fig. 10a–d). Correspondingly, quantitative PCR with reverse transcription analysis of a previously described set of cytokines and inflammatory genes[11] showed reduced mRNA expression in the lungs of hamsters treated with COV2-2130/COV2-2196 (Extended Data Fig. 10e–h). Consensus sequencing of the RBD region of viral RNA samples from the lungs of hamsters treated with COV2-2130/COV2-2196 did not show evidence of mutation or escape (Supplementary Table 3). When the

lower 320-μg dose of COV2-2130/COV2-2196 was administered, we observed a trend towards protection against weight loss in hamsters infected with WA1/2020 D614G and Wash-B.1.351. Consistent with a partially protective phenotype, hamsters treated with the lower 320-μg dose of COV2-2130/COV2-2196 and inoculated with either WA1/2020 D614G or Wash-B.1.351 showed a trend towards reduced viral RNA in the lungs at 4 days after infection and markedly diminished (about 10^4- to 10^5-fold) levels of infectious virus as determined by plaque assay (Extended Data Fig. 10j, k). The reduction in lung viral load conferred by the lower dose of COV2-2130/COV2-2196 corresponded with diminished inflammatory gene expression after infection with either WA1/2020 D614G or Wash-B.1.351 (Extended Data Fig. 10m–p). In contrast to the protection seen in the lung, differences in viral RNA were not observed in nasal washes between COV2-2130/COV2-2196 and isotype control mAb-treated hamsters, regardless of the infecting strain (Extended Data Fig. 10l). Sequencing of the RBD of viral RNA from the lungs of COV2-2130/COV2-2196 or isotype mAb-treated hamsters also did not detect evidence of escape mutation selection after infection (Supplementary Table 3). Overall, these studies in hamsters with near-threshold dosing of the COV2-2130/COV2-2196 mAb cocktail establish protection and an absence of rapid escape against SARS-CoV-2 containing spike proteins from historical or variant strains.

Therapeutic efficacy against variants

As mAbs are being developed clinically as therapeutic agents, we assessed their post-exposure efficacy against the SARS-CoV-2 strain expressing the B.1.351 spike protein using K18-hACE2 mice. We administered a single, higher (200-μg; about 10 mg kg^{-1}) dose of COV2-2130/COV2-2196, S309/S2E12, REGN10933/REGN10987 or 2B04/47D11 by intraperitoneal injection one day after inoculation with WA1/2020 N501Y/D614G (Fig. 3a–c) or Wash-B.1.351 (Fig. 3d–f). Compared to the control mAb-treated mice, which lost at least 15% of their starting weight over the 6 days of the experiment, each of these mAb cocktails prevented weight loss induced by WA1/2020 N501Y/D614G or Wash-B.1.351 infection (Fig. 3a, d). Histopathological analysis of lung sections from control mAb-treated mice showed interstitial oedema, immune cell infiltration and collapsed alveolar spaces, consistent with the inflammation induced by SARS-CoV-2 infection (Extended Data Fig. 11). By contrast, COV2-2130/COV2-2196-, S309/S2E12-, REGN10933/REGN10987- and 2B04/47D11-treated mice showed reduced or minimal lung pathology. COV2-2130/COV2-2196, S309/S2E12 and REGN10933/REGN10987 mAb cocktail treatments resulted in reduced infectious virus and viral RNA levels in lung homogenates, and viral RNA levels in nasal washes and brain homogenates from mice infected with either WA1/2020 N501Y/D614G or Wash-B.1.351 (Fig. 3b, c, e, f, Extended Data Figs. 3g, h, 12). By comparison, although the 2B04/47D11 mAb cocktail reduced viral RNA levels in the lungs, it showed less protection in the nasal washes of WA1/2020-N501Y/D614G- or Wash-B.1.351-infected mice. Although neutralizing capacity correlated with lung viral burden when mAbs were administered as prophylaxis, this association was less direct when mAbs were given in the post-exposure setting (Extended Data Fig. 8). This result was not entirely unexpected, as effector functions of some mAbs are required for optimal activity when given as post-exposure therapy[11,16]. Indeed, recent studies with influenza and SARS-CoV-2 neutralizing antibodies suggest that Fc engagement mitigates inflammation, improves respiratory mechanics and promotes viral clearance in the lung[11,17].

With the emergence of several SARS-CoV-2 variants, it remains uncertain whether vaccines and antibody-based therapies will lose efficacy[18]. Cell-culture-based studies have shown that several of the mutations in variant strains (especially those at positions 452 and 484) result in reduced neutralization by antibodies derived from infected or vaccinated individuals[1–3,19,20]. Here we evaluated antibodies forming the basis of five mAb therapies in clinical development for in vivo efficacy

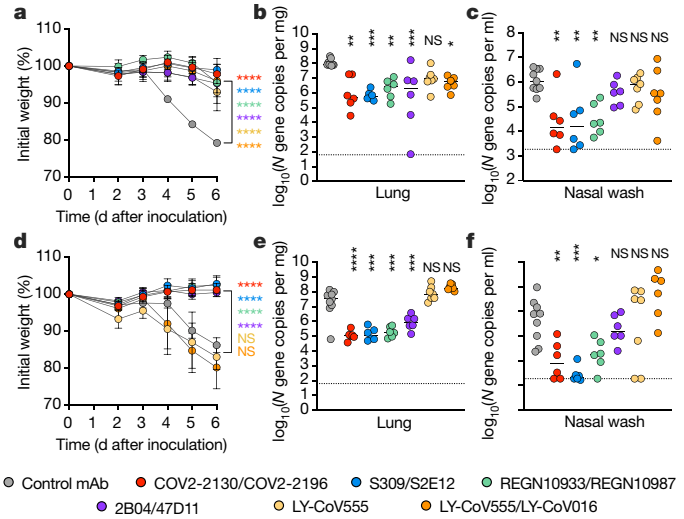

Fig. 3 | Post-exposure antibody therapy against SARS-CoV-2 variants in K18-hACE2 mice. a–f, Eight-to-ten-week-old female and male K18-hACE2 transgenic mice were administered 10^3 FFU of the SARS-CoV-2 N501Y/D614G (**a**–**c**) or Wash-B.1.351 (**d**–**f**) strains by intranasal inoculation. One day later, mice received 200 μg (about 10 mg kg^{-1}) of the indicated mAb treatment by intraperitoneal injection. Tissues were collected at six days after infection. **a**, **d**, Weight change after infection with SARS-CoV-2 (mean ± s.e.m.; in order from left to right $n = 15, 6, 6, 6, 6, 7$ and 7 (**a**, **d**) mice per group, two experiments; one-way ANOVA with Dunnett's test of area under the curve. NS, not significant, ****$P < 0.0001$). Viral RNA levels in the lung (**b**, **e**) and nasal wash (**c**, **f**) (line indicates median; in order from left to right $n = 7, 6, 6, 6, 6, 7$ and 7 (**b**); $n = 9, 6, 6, 6, 6, 7$ and 7 (**c**, **e**, **f**) mice per group, 2 experiments; one-way ANOVA with Dunnett's test with comparison to control mAb. NS, not significant, ****$P < 0.0001$; **$P = 0.0014$ (left) and 0.0088 (right), ***$P = 0.0007$ (left) and 0.0003 (right) (**b**); **$P = 0.0026$ (left), 0.0041 (middle) and 0.0049 (right) (**c**); **$P = 0.0049$, ***$P = 0.0004$ (**e**); **$P = 0.0094$, ***$P = 0.0005$, *$P = 0.0442$ (**f**)). Dotted line indicates the limit of detection of the assay.

against infection by SARS-CoV-2 variants. Monotherapy with LY-CoV555, an antibody that corresponds to bamlanivimab[21], showed complete neutralization escape in cell culture and did not confer protection against viruses containing E484 substitutions. By contrast, all cocktails of two neutralizing mAbs conferred protection to varying degrees, even if one of the constituent mAbs showed reduced activity owing to resistance. Moreover, the higher doses of mAbs used in patients (for example, about 35 mg kg^{-1} for casirivimab and imdevimab (corresponding to the REGN mAbs)) could compensate for loss in neutralization potency. Generally, in mice and hamsters, mAb-mediated protection was better in the lung than in nasal washes, possibly because IgG levels in the respiratory mucosa are lower than in plasma[22,23].

In our study, combination therapy with several mAbs was protective in mice and hamsters against variant strains, which highlights the importance of using multiple mAbs that recognize distinct epitopes (rather than monotherapy) to control SARS-CoV-2 infection. Indeed, the Emergency Use Authorization for bamlanivimab (LY-CoV555) as monotherapy was revoked, as the antibody does not reduce SARS-CoV-2 infection of several variants of concern[2,24,25]; instead, a combination of bamlanivimab (LY-CoV555) and etesevimab (LY-CoV016) is recommended, even though strains that contain E484 and K417 mutations (such as B.1.351, B.1.1.28, B.1.617.1 and B.1.526) will probably have resistance to both mAb components[2,26] (Extended Data Fig. 13). Indeed, in K18-hACE2 mice, we found that LY-CoV555/LY-CoV016 had therapeutic activity against WA1/2020 N501Y/D614G (Fig. 3a–c) but not against Wash-B.1.351 (Fig. 3d–f). This failure of protection occurred because both of the mAbs in the cocktail lost neutralizing activity. Other cocktails may fare better against variants of concern as long as one of the

mAbs in each pair retains substantial inhibitory activity. Beyond a loss of potency against already circulating resistant variants, antibody monotherapy can be compromised within an individual by rapid selection of escape mutations. Consistent with this idea, in other animal experiments with SARS-CoV-2, we observed the emergence of resistance against antibody monotherapy, resulting in the accumulation of mutations at RBD residues 476, 477, 484, or 487 (ref. [27], and M.S.D., unpublished data). Despite amplifying sequences from 99 brain, nasal wash and lung samples from mice and hamsters treated with the different mAb combinations in this study, we did not detect a single escape mutant. Combination mAb treatment may prevent escape through synergistic interactions in vivo or by driving selection of mutants with compromised fitness.

At the lower doses of the mAbs we tested, we observed some differences in mAb cocktail efficacy between rodent models, which could be due to host variation, viral variation or small differences in antibody levels. For example, mutations in the RBD can affect mAb binding as well as ACE2 binding[28]. Mutation at position 501 of the spike is of particular interest, as it enables mouse adaptation[12,13] and is present in several variants of concern. The N501Y change associated with infection of conventional laboratory mice could facilitate virus engagement with mouse ACE2 or possibly other putative receptors. Beyond this, polymorphisms in or differences of expression of host receptors on key target cells also could affect SARS-CoV-2 infection in different hosts and the inhibitory effects of neutralizing antibodies. This complexity of antibody–spike protein–receptor interactions probably explains some of the variation in protection between K18-hACE2 mice, 129S2 mice and hamsters. Alternatively, the pharmacokinetics of human antibodies could vary between animals and affect efficacy. We observed small differences in serum antibody levels in the context of viral challenge that could affect relative protection (Supplementary Table 4).

Previous studies with pseudoviruses and authentic SARS-CoV-2 containing variant substitutions have suggested that adjustments to therapeutic antibody regimens might be necessary[1,2,29–31]. Although our studies with variant strains in vivo suggest that this conclusion probably holds for mAb monotherapy, four different mAb combinations performed well even when a virus was fully resistant to one mAb component. Thus, our results suggest that—as previously described for the historical WA1/2020 strain[32]—many, but not all, combination therapies with neutralizing mAbs should retain efficacy against emerging SARS-CoV-2 variants.

Online content

Any methods, additional references, Nature Research reporting summaries, source data, extended data, supplementary information, acknowledgements, peer review information; details of author contributions and competing interests; and statements of data and code availability are available at https://doi.org/10.1038/s41586-021-03720-y.

1. Chen, R. E. et al. Resistance of SARS-CoV-2 variants to neutralization by monoclonal and serum-derived polyclonal antibodies. *Nat. Med.* **27**, 717–726 (2021).
2. Wang, P. et al. Antibody resistance of SARS-CoV-2 variants B.1.351 and B.1.1.7. *Nature* **593**, 130–135 (2021).
3. Wang, Z. et al. mRNA vaccine-elicited antibodies to SARS-CoV-2 and circulating variants. *Nature* **592**, 616–622 (2021).
4. Wibmer, C. K. et al. SARS-CoV-2 501Y.V2 escapes neutralization by South African COVID-19 donor plasma. *Nat. Med.* **27**, 622–625 (2021).
5. Tada, T. et al. Convalescent-phase sera and vaccine-elicited antibodies largely maintain neutralizing titer against global SARS-CoV-2 variant spikes. *mBio* **12**, https://doi.org/10.1128/mBio.00696-21 (2021).
6. Xie, X. et al. Neutralization of SARS-CoV-2 spike 69/70 deletion, E484K and N501Y variants by BNT162b2 vaccine-elicited sera. *Nat. Med.* **27**, 620–621 (2021).
7. Johnson, B. A. et al. Loss of furin cleavage site attenuates SARS-CoV-2 pathogenesis. *Nature* **591**, 293–299 (2021).
8. Deng X. et al. Transmission, infectivity, and neutralization of a spike L452R SARS-CoV-2 variant. *Cell* **184**, 3426–3437 (2021).
9. Winkler, E. S. et al. SARS-CoV-2 infection of human ACE2-transgenic mice causes severe lung inflammation and impaired function. *Nat. Immunol.* **21**, 1327–1335 (2020).
10. McCray, P. B. Jr et al. Lethal infection of K18-hACE2 mice infected with severe acute respiratory syndrome coronavirus. *J. Virol.* **81**, 813–821 (2007).
11. Winkler, E. S. et al. Human neutralizing antibodies against SARS-CoV-2 require intact Fc effector functions for optimal therapeutic protection. *Cell* **184**, 1804–1820 (2021).
12. Rathnasinghe, R. et al. The N501Y mutation in SARS-CoV-2 spike leads to morbidity in obese and aged mice and is neutralized by convalescent and post-vaccination human sera. Preprint at https://doi.org/10.1101/2021.01.19.21249592 (2021).
13. Gu, H. et al. Adaptation of SARS-CoV-2 in BALB/c mice for testing vaccine efficacy. *Science* **369**, 1603–1607 (2020).
14. Zhou, D. et al. Robust SARS-CoV-2 infection in nasal turbinates after treatment with systemic neutralizing antibodies. *Cell Host Microbe* **29**, 551–563 (2021).
15. Andreano, E. et al. Extremely potent human monoclonal antibodies from COVID-19 convalescent patients. *Cell* **184**, 1821–1835 (2021).
16. Schäfer, A. et al. Antibody potency, effector function, and combinations in protection and therapy for SARS-CoV-2 infection in vivo. *J. Exp. Med.* **218**, e20201993 (2021).
17. Bournazos, S., Corti, D., Virgin, H. W. & Ravetch, J. V. Fc-optimized antibodies elicit CD8 immunity to viral respiratory infection. *Nature* **588**, 485–490 (2020).
18. Cobey, S., Larremore, D. B., Grad, Y. H. & Lipsitch, M. Concerns about SARS-CoV-2 evolution should not hold back efforts to expand vaccination. *Nat. Rev. Immunol.* **21**, 330–335 (2021).
19. Shen, X. et al. Neutralization of SARS-CoV-2 variants B.1.429 and B.1.351. *N. Engl. J. Med.* (2021).
20. .McCallum, M. et al. SARS-CoV-2 immune evasion by variant B.1.427/B.1.429. Preprint at https://doi.org/10.1101/2021.03.31.437925 (2021).
21. ACTIV-3/TICO LY-CoV555 Study Group. A neutralizing monoclonal antibody for hospitalized patients with Covid-19. *N. Engl. J. Med.* **384**, 905–914 (2021).
22. Reynolds, H. Y. Immunoglobulin G and its function in the human respiratory tract. *Mayo Clin. Proc.* **63**, 161–174 (1988).
23. Borrok, M. J. et al. Enhancing IgG distribution to lung mucosal tissue improves protective effect of anti-*Pseudomonas aeruginosa* antibodies. *JCI Insight* **3**, e97844 (2018).
24. Gottlieb, R. L. et al. Effect of bamlanivimab as monotherapy or in combination with etesevimab on viral load in patients with mild to moderate COVID-19: a randomized clinical trial. *J. Am. Med. Assoc.* **325**, 632–644 (2021).
25. Wang, P. et al. Increased resistance of SARS-CoV-2 variant P.1 to antibody neutralization. *Cell Host Microbe* **29**, 747–751 (2021).
26. Starr, T. N., Greaney, A. J., Dingens, A. S. & Bloom, J. D. Complete map of SARS-CoV-2 RBD mutations that escape the monoclonal antibody LY-CoV555 and its cocktail with LY-CoV016. *Cell Rep. Med.* **2**, 100255 (2021).
27. Schmitz, A. J. et al. A public vaccine-induced human antibody protects against SARS-CoV-2 and emerging variants. Preprint at https://doi.org/10.1101/2021.03.24.436864 (2021).
28. Tian, F. et al. Mutation N501Y in RBD of spike protein strengthens the interaction between COVID-19 and its receptor ACE2. Preprint at https://doi.org/10.1101/2021.02.14.431117 (2021).
29. Graham, C. et al. Neutralization potency of monoclonal antibodies recognizing dominant and subdominant epitopes on SARS-CoV-2 spike is impacted by the B.1.1.7 variant. *Immunity* **54**, 1276–1289 (2021).
30. Rees-Spear, C. et al. The effect of spike mutations on SARS-CoV-2 neutralization. *Cell Rep.* **34**, 108890 (2021).
31. Zhou, D. et al. Evidence of escape of SARS-CoV-2 variant B.1.351 from natural and vaccine-induced sera. *Cell* **184**, 2348–2361 (2021).
32. Baum, A. et al. Antibody cocktail to SARS-CoV-2 spike protein prevents rapid mutational escape seen with individual antibodies. *Science* **369**, 1014–1018 (2020).
33. Goddard, T. D. et al. UCSF ChimeraX: meeting modern challenges in visualization and analysis. *Protein Sci.* **27**, 14–25 (2018).

Methods

No statistical methods were used to predetermine sample size. The experiments were not randomized, and investigators were not blinded to allocation during experiments and outcome assessment.

Cells

Vero-TMPRSS2[34] and Vero cells expressing human ACE2 and TMPRRS2 (Vero-hACE2-TMPRRS2)[1] cells were cultured at 37 °C in Dulbecco's modified Eagle medium (DMEM) supplemented with 10% fetal bovine serum (FBS), 10 mM HEPES pH 7.3, 1 mM sodium pyruvate, 1× non-essential amino acids and 100 U ml^{-1} of penicillin–streptomycin. Vero-TMPRSS2 cells were supplemented with 5 μg ml^{-1} of blasticidin. Vero-hACE2-TMPRSS2 cells were supplemented with 10 μg ml^{-1} of puromycin. All cells routinely tested negative for mycoplasma using a PCR-based assay.

Viruses

The WA1/2020 recombinant strains with substitutions (D614G or N501Y/D614G) were obtained from an infectious cDNA clone of the 2019n-CoV/USA_WA1/2020 strain, as previously described[35]. The B.1.351- and B.1.1.28-variant spike genes were introduced into the WA1/2020 backbone as previously described to create chimeric SARS-CoV-2[1]. The B.1.1.7, B.1.429, B.1.351 and B.1.526 (S477N or E484K variant) isolates were obtained from nasopharyngeal isolates. The B.1.617.1 variant was plaque-purified from a midturbinate nasal swab and passaged twice on Vero-TMPRSS2 cells, as previously described[36]. All viruses were passaged once in Vero-TMPRSS2 cells and subjected to next-generation sequencing as previously described[1] to confirm the introduction and stability of substitutions (Supplementary Table 1). Substitutions for each variant were as follows: B.1.1.7: deletion of 69 and 70 and 144 and 145, N501Y, A570D, D614G, P681H, T716I, S982A, and D1118H; B.1.351: D80A, T95I, D215G, deletion of 242-244, K417N, E484K, N501Y, D614G, and A701V; B.1.1.28: L18F, T20N, P26S, D138Y, R190S, K417T, E484K, N501Y, D614G, H655Y, and T1027I; B.1.429: S13I, W152C, L452R, and D614G; B.1.617.1: G142D, E154K, L452R, E484Q, D614G, P681R, Q1071H, and H1101D; and B.1.526 (S477N or E484K variant): L5F, T95I, D253G, S477N, E484K, D614G, and A701V or Q957R. All virus experiments were performed in an approved biosafety level 3 facility.

mAb purification

The mAbs studied in this paper (COV2-2196, COV2-2130, S309, S2E12, 2B04, 47D11, REGN10933, REGN10987, LY-CoV555 and LY-CoV016) have previously been described[32,37–43]. COV2-2196 and COV2-2130 mAbs were produced after transient transfection using the Gibco ExpiCHO Expression System (ThermoFisher Scientific) following the manufacturer's protocol. Culture supernatants were purified using HiTrap MabSelect SuRe columns (Cytiva, (formerly GE Healthcare Life Sciences)) on an AKTA Pure chromatographer (GE Healthcare Life Sciences). Purified mAbs were buffer-exchanged into PBS, concentrated using Amicon Ultra-4 50-kDa centrifugal filter units (Millipore Sigma) and stored at −80 °C until use. Purified mAbs were tested for endotoxin levels (found to be less than 30 EU per mg IgG). Endotoxin testing was performed using the PTS201F cartridge (Charles River), with a sensitivity range from 10 to 0.1 EU per ml, and an Endosafe Nexgen-MCS instrument (Charles River). S309, S2E12, REGN10933, REGN10987, LY-CoV016 and LY-CoV555 mAb proteins were produced in CHOEXPI cells and affinity-purified using HiTrap Protein A columns (GE Healthcare, HiTrap mAb select Xtra no. 28-4082-61). Purified mAbs were suspended into 20 mM histidine, 8% sucrose, pH 6.0. The final products were sterilized by filtration through 0.22-μm filters and stored at 4 °C.

Mouse experiments

Animal studies were carried out in accordance with the recommendations in the Guide for the Care and Use of Laboratory Animals of the National Institutes of Health. The protocols were approved by the Institutional Animal Care and Use Committee at the Washington University School of Medicine (assurance number A3381–01). Virus inoculations were performed under anaesthesia that was induced and maintained with ketamine hydrochloride and xylazine, and all efforts were made to minimize animal suffering.

Heterozygous K18-hACE2 C57BL/6J mice (strain: 2B6.Cg-Tg(K18-ACE2)2Prlmn/J) and 129 mice (strain: 129S2/SvPasCrl) were obtained from The Jackson Laboratory and Charles River Laboratories, respectively. Mice were housed in groups and fed standard chow diets. Six-to-ten-week-old mice of both sexes were administered 10^3 or 10^5 FFU of the respective SARS-CoV-2 strain by intranasal administration. In vivo studies were not blinded, and mice were randomly assigned to treatment groups. No sample-size calculations were performed to power each study. Instead, sample sizes were determined on the basis of previous in vivo virus challenge experiments.

For antibody prophylaxis and therapeutic experiments, mice were administered the indicated mAb dose by intraperitoneal injection one day before or after intranasal inoculation with the indicated SARS-CoV-2 strain.

Hamster experiments

Six-month-old male Syrian hamsters were purchased from Charles River Laboratories and housed in microisolator units. All hamsters were allowed free access to food and water and cared for under United States Department of Agriculture (USDA) guidelines for laboratory animals. Hamsters were administered by intraperitoneal injection mAbs COV2-2130 and COV2-2196 or isotype control (4 or 10 mg kg^{-1}, depending on the experiment). One day later, hamsters were given 5×10^5 FFU of indicated SARS-CoV-2 strain by the intranasal route in a final volume of 100 μl. All hamsters were monitored for body weight loss until being humanely euthanized at four days after infection. Nasal swabs were collected at three days after infection. All procedures were approved by the Washington University School of Medicine (assurance number A3381–01). Virus inoculations and antibody transfers were performed under anaesthesia that was induced and maintained with 5% isoflurane. All efforts were made to minimize animal suffering.

Focus reduction neutralization test

Serial dilutions of mAbs (starting at 10 μg ml^{-1} dilution) were incubated with 10^2 FFU of different strains or variants of SARS-CoV-2 for 1 h at 37 °C. Antibody–virus complexes were added to Vero-TMPRSS2 cell monolayers in 96-well plates and incubated at 37 °C for 1 h. Subsequently, cells were overlaid with 1% (w/v) methylcellulose in MEM. Plates were collected 30 h later by removing overlays and fixed with 4% PFA in PBS for 20 min at room temperature. Plates were washed and sequentially incubated with an oligoclonal pool of SARS2-2, SARS2-11, SARS2-16, SARS2-31, SARS2-38, SARS2-57 and SARS2-71[44] anti-S antibodies and HRP-conjugated goat anti-mouse IgG (Sigma, 12-349) in PBS supplemented with 0.1% saponin and 0.1% bovine serum albumin. SARS-CoV-2-infected cell foci were visualized using TrueBlue peroxidase substrate (KPL) and quantitated on an ImmunoSpot microanalyzer (Cellular Technologies).

Measurement of viral burden

Tissues were weighed and homogenized with zirconia beads in a MagNA Lyser instrument (Roche Life Science) in 1000 μl of DMEM medium supplemented with 2% heat-inactivated FBS. Tissue homogenates were clarified by centrifugation at 10,000 rpm for 5 min and stored at −80 °C. RNA was extracted using the MagMax mirVana Total RNA isolation kit (Thermo Fisher Scientific) on the Kingfisher Flex extraction robot (Thermo Fisher Scientific). RNA was reverse-transcribed and amplified using the TaqMan RNA-to-CT 1-Step Kit (Thermo Fisher Scientific). Reverse transcription was carried out at 48 °C for 15 min followed by 2 min at 95 °C. Amplification was accomplished over 50 cycles as

follows: 95 °C for 15 s and 60 °C for 1 min. Copies of SARS-CoV-2 *N* gene RNA in samples were determined using a previously published assay[45]. In brief, a TaqMan assay was designed to target a highly conserved region of the *N* gene (forward primer: ATGCTGCAATCGTGCTACAA; reverse primer: GACTGCCGCCTCTGCTC; probe: /56-FAM/TCAAGGAAC/ZEN/AACATTGCCAA/3IABkFQ/). This region was included in an RNA standard to allow for copy number determination down to 10 copies per reaction. The reaction mixture contained final concentrations of primers and probe of 500 and 100 nM, respectively.

Plaque assay

Vero-hACE2-TMPRSS2 cells were seeded at a density of 1×10^5 cells per well in 24-well tissue culture plates. The following day, medium was removed and replaced with 200 µl of material to be titrated diluted serially in DMEM supplemented with 2% FBS. One hour later, 1 ml of methylcellulose overlay was added. Plates were incubated for 72 h, then fixed with 4% paraformaldehyde (final concentration) in PBS for 20 min. Plates were stained with 0.05% (w/v) crystal violet in 20% methanol and washed twice with distilled, deionized water.

Cytokine and chemokine protein measurements

Lung homogenates were incubated with Triton-X-100 (1% final concentration) for 1 h at room temperature to inactivate SARS-CoV-2. Homogenates then were analysed for cytokines and chemokines by Eve Technologies using their Mouse Cytokine Array/Chemokine Array 31-Plex (MD31) platform.

Lung histology

Animals were euthanized before harvest and fixation of tissues. Lungs were inflated with about 2 ml of 10% neutral buffered formalin using a 3-ml syringe and catheter inserted into the trachea and kept in fixative for 7 days. Tissues were embedded in paraffin, and sections were stained with haematoxylin and eosin. Images were captured using the Nanozoomer (Hamamatsu) at the Alafi Neuroimaging Core at Washington University.

Statistical analysis

All statistical tests were performed as described in the indicated figure legends using Prism 8.0. Statistical significance was determined using an ordinary one-way ANOVA with Dunnett's post-test when comparing three or more groups. The number of independent experiments used are indicated in the relevant figure legends.

Reporting summary

Further information on research design is available in the Nature Research Reporting Summary linked to this paper.

Data availability

All data supporting the findings of this study are available within the paper and are available from the corresponding author upon request. Source data are provided with this paper.

34. Zang, R. et al. TMPRSS2 and TMPRSS4 promote SARS-CoV-2 infection of human small intestinal enterocytes. *Sci. Immunol.* **5**, eabc3582 (2020).
35. Plante, J. A. et al. Spike mutation D614G alters SARS-CoV-2 fitness. *Nature* **592**, 116–121 (2021).
36. Edara, V.-V. et al. Infection and vaccine-induced neutralizing antibody responses to the SARS-CoV-2 B.1.617.1 variant. Preprint at https://doi.org/10.1101/2021.05.09.443299 (2021).
37. Zost, S. J. et al. Rapid isolation and profiling of a diverse panel of human monoclonal antibodies targeting the SARS-CoV-2 spike protein. *Nat. Med.* **26**, 1422–1427 (2020).
38. Pinto, D. et al. Cross-neutralization of SARS-CoV-2 by a human monoclonal SARS-CoV antibody. *Nature* **583**, 290–295 (2020).
39. Tortorici, M. A. et al. Ultrapotent human antibodies protect against SARS-CoV-2 challenge via multiple mechanisms. *Science* **370**, 950–957 (2020).
40. Alsoussi, W. B. et al. A potently neutralizing antibody protects mice against SARS-CoV-2 infection. *J. Immunol.* **205**, 915–922 (2020).
41. Baum, A. et al. REGN-COV2 antibodies prevent and treat SARS-CoV-2 infection in rhesus macaques and hamsters. *Science* **370**, 1110–1115 (2020).
42. Jones, B. E. et al. The neutralizing antibody, LY-CoV555, protects against SARS-CoV-2 infection in nonhuman primates. *Sci. Transl. Med.* **13**, eabf1906 (2020).
43. Shi, R. et al. A human neutralizing antibody targets the receptor-binding site of SARS-CoV-2. *Nature* **584**, 120–124 (2020).
44. Liu, Z. et al. Identification of SARS-CoV-2 spike mutations that attenuate monoclonal and serum antibody neutralization. *Cell Host Microbe* **29**, 477–488 (2021).
45. Case, J. B., Bailey, A. L., Kim, A. S., Chen, R. E. & Diamond, M. S. Growth, detection, quantification, and inactivation of SARS-CoV-2. *Virology* **548**, 39–48 (2020).

Acknowledgements This study was supported by grants and contracts from NIH (R01 AI157155, U01 AI151810, U01 AI141990, R01 AI118938, 75N93019C00051, HHSN272201400006C, HHSN272201400008C, HHSN75N93019C00074 and HHSN272201400006C), the Children's Discovery Institute (PDII2018702), the Defense Advanced Research Project Agency (HR0011-18-2-0001), the Dolly Parton COVID-19 Research Fund at Vanderbilt University, a grant from Fast Grants, Mercatus Center, George Mason University and the Future Insight Prize (Merck KGaA; to J.E.C. Jr). J.B.C. is supported by a Helen Hay Whitney Foundation postdoctoral fellowship, E.S.W. is supported by F30 AI152327 and S.J.Z. is supported by NIH grant T32 AI095202. P.-Y.S. is supported by the Sealy & Smith Foundation, the Kleberg Foundation, the John S. Dunn Foundation, the Amon G. Carter Foundation, the Gilson Longenbaugh Foundation and the Summerfield Robert Foundation. We thank R. Nargi, R. Carnahan, T. Tan and L. Schimanski for assistance and generosity with mAb generation and purification; S. Tahan for some of the deep sequencing analysis; and the Pulmonary Morphology Core at Washington University School of Medicine for tissue sectioning and slide imaging.

Author contributions R.E.C. performed and analysed neutralization assays. R.E.C., E.S.W. and J.B.C. performed mouse experiments. R.E.C., E.S.W., J.B.C., B.Y. and S. Shrihari performed viral burden analyses. X.X. generated the recombinant SARS-CoV-2 viruses. R.E.C. and L.A.V. propagated and validated SARS-CoV-2 viruses. L.D., S.A.H. and D.W. performed deep sequencing analysis. I.D.A. and S. Stumpf performed Sanger sequencing analyses. T.L.D., T.L.B. and A.C.M.B. performed the hamster studies. T.L.D. and A.J. performed viral burden and inflammatory gene analysis. J.M.E. and D.H.F. performed structural analysis. Z.L. generated escape mutants. E.S.W. quantified serum antibody concentrations. J.B.C. and T.L.B. performed plaque assays. D.C., P.G., S.J.Z., W.B.S. Jr, J.E.C. Jr, A.H.E. and L.P. provided mAbs. M.S.S., M.E.D.-G., P.-Y.S., M.G.K., R.A. and C.Y.C. provided SARS-CoV-2 strains. P.-Y.S., A.H.E., D.C., S.P.J.W., A.C.M.B. and M.S.D. obtained funding and supervised the research. R.E.C., E.S.W., J.B.C. and M.S.D. wrote the initial draft, with the other authors providing editorial comments.

Competing interests M.S.D. is a consultant for Inbios, Vir Biotechnology, Fortress Biotech and Carnival Corporation, and on the Scientific Advisory Boards of Moderna and Immunome. The laboratory of M.S.D. has received funding support in sponsored research agreements from Moderna, Vir Biotechnology, Kaleido and Emergent BioSolutions. M.S.S. is on the Advisory Board of Moderna. J.E.C. Jr has served as a consultant for Eli Lilly and Luna Biologics, is a member of the Scientific Advisory Boards of CompuVax and Meissa Vaccines, and is Founder of IDBiologics. The laboratory of J.E.C. Jr has received sponsored research agreements from Takeda, AstraZeneca and IDBiologics. Vanderbilt University (J.E.C. Jr) and Washington University (A.H.E., D.H.F., J.B.C., A.C.M.B. and M.S.D.) have applied for patents related to antibodies in this paper. The laboratory of A.H.E. has received funding support in sponsored research agreements from AbbVie Inc. and Emergent BioSolutions. The laboratory of A.C.M.B. has received funding support in sponsored research agreements from AI Therapeutics, GreenLight Biosciences, AbbVie, and Nano Targeting & Therapy Biopharma. The laboratory of P.-Y.S. has received sponsored research agreements from Pfizer, Gilead, Merck and IGM Sciences Inc. D.C. and L.P. are employees of Vir Biotechnology and may hold equity in Vir Biotechnology. L.P. is a former employee and may hold equity in Regeneron Pharmaceuticals. W.B.S. Jr is an employee of AbbVie and may hold equity.

Additional information

Supplementary information The online version contains supplementary material available at https://doi.org/10.1038/s41586-021-03720-y.

Correspondence and requests for materials should be addressed to M.S.D.

Peer review information *Nature* thanks the anonymous reviewers for their contribution to the peer review of this work. Peer reviewer reports are available.

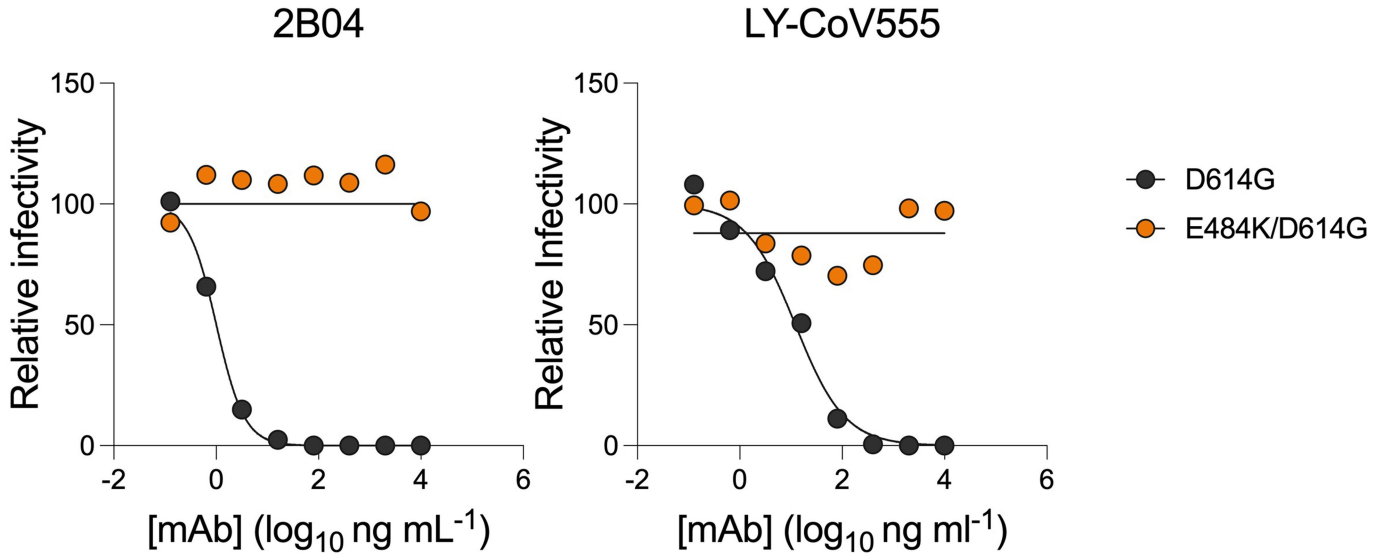

Extended Data Fig. 1 | Neutralization curves with mAbs and variant SARS-CoV-2 strains. Anti-SARS-CoV-2 human mAbs were tested for inhibition of infection of the indicated viruses on Vero-TMPRSS2 cells using a focus reduction neutralization test. One representative experiment of two performed in duplicate is shown.

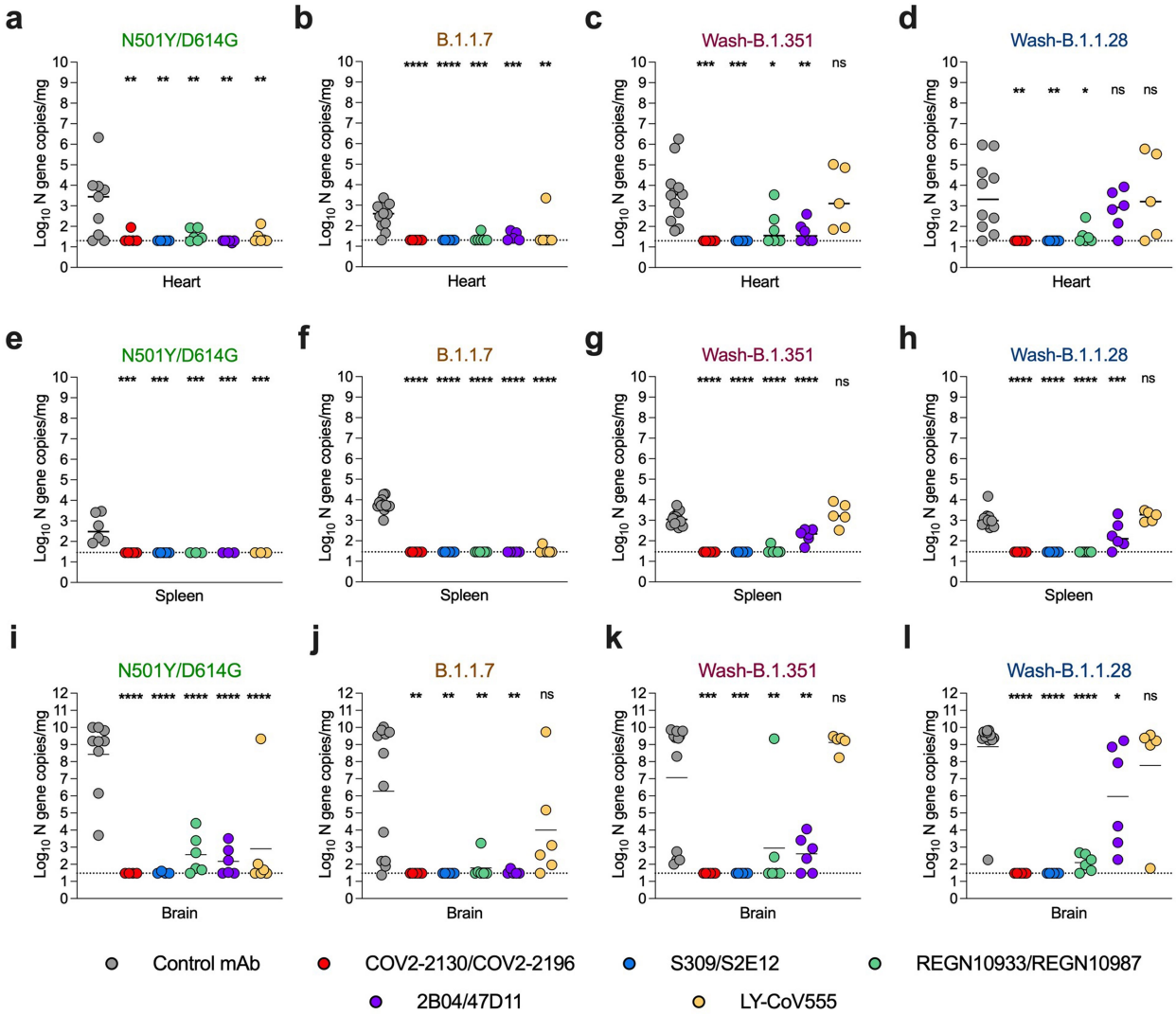

Extended Data Fig. 2 | SARS-CoV-2 variant infection after antibody prophylaxis of K18-hACE2 mice. a–**l**, Eight-to-ten-week-old female and male K18-hACE2 transgenic mice received 40 μg of the indicated mAb treatment by intraperitoneal injection one day before intranasal challenge with 10^3 FFU of the indicated SARS-CoV-2 strain. At 6 days after infection, viral RNA levels in the heart (**a**–**d**), spleen (**e**–**h**) and brain (**i**–**l**) were measured (line indicates median; in order from left to right $n = 9, 5, 5, 6, 6$ and 6 (**a**); $n = 12, 6, 6, 6, 5$, and 6 (**b**, **c**, **f**, **g**, **j**, **k**); $n = 10, 6, 6, 6, 6$ and 5 (**d**, **h**); $n = 6, 5, 5, 3, 3$ and 3 (**e**); $n = 9, 4, 4, 6, 6$ and 6 (**i**); $n = 11, 6, 6, 6, 6$ and 5 (**l**) mice per group, two experiments; one-way ANOVA with Dunnett's test with comparison to control mAb: ns, not significant, $^{****}P < 0.0001$; in order from left to right $^{**}P = 0.0066, 0.0032, 0.0080, 0.0016$ and 0.0052 (**a**); $^{***}P = 0.0002$, $^{**}P = 0.0017$ and 0.0052 (**b**); $^{***}P = 0.0004$ and 0.0004, $^{*}P = 0.0140$, $^{**}P = 0.0043$ (**c**); $^{**}P = 0.0080$ and 0.0080, $^{*}P = 0.0226$ (**d**); $^{***}P = 0.0001, 0.0001, 0.0008, 0.0008$ and 0.0008 (**e**); $^{***}P = 0.0008$ (**h**); $^{**}P = 0.0014, 0.0014, 0.0029$ and 0.0032 (**j**); $^{***}P = 0.0002$ and 0.0002, $^{**}P = 0.0061$ and 0.0028 (**k**); $^{*}P = 0.0371$ (**l**)). Dotted line indicates the limit of detection of the assay.

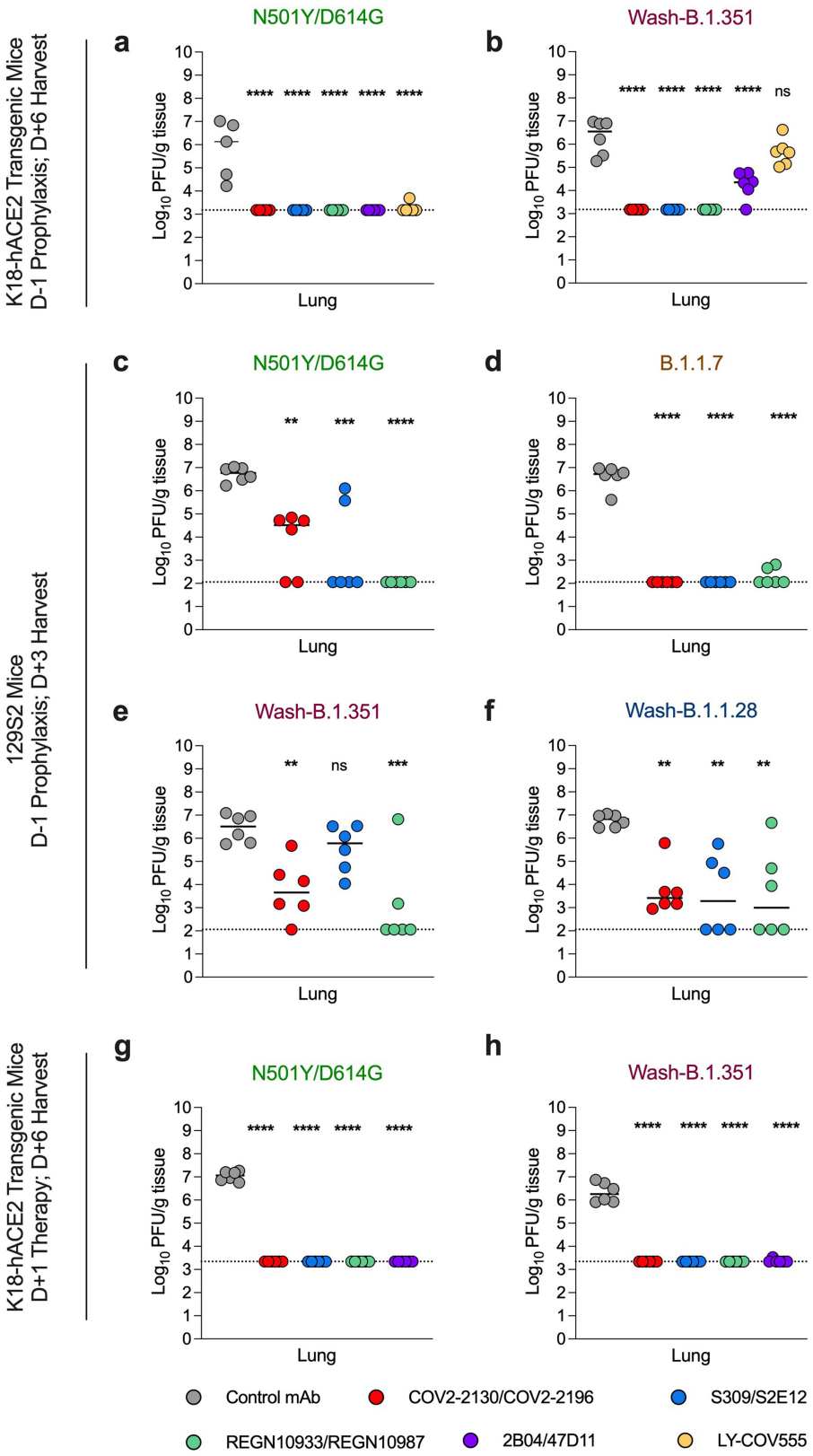

Extended Data Fig. 3 | See next page for caption.

Extended Data Fig. 3 | Reduced infectious virus in the lungs of antibody-treated mice. a, **b**, Eight-to-ten-week-old female and male K18-hACE2 transgenic mice received 40 μg (about 2 mg kg^{-1}) of the indicated mAb treatment by intraperitoneal injection one day before intranasal inoculation with 10^3 FFU of the indicated SARS-CoV-2 strain. Tissues were collected at six days after infection. **c**–**f**, Six-to-seven-week-old female and male immunocompetent 129S2 mice received 40 μg (about 2 mg kg^{-1}) of the indicated mAb treatment by intraperitoneal injection one day before intranasal inoculation with 10^3 FFU of WA1/2020 N501Y/D614G, Wash-B.1.351 or Wash-B.1.1.28 and 10^5 FFU of B.1.1.7. Tissues were collected at three days after infection. **g**, **h**, Eight-to-ten-week-old female and male K18-hACE2 transgenic mice were administered 10^3 FFU of the indicated SARS-CoV-2 strain by intranasal inoculation. One day later, mice received 200 μg (about 10 mg kg^{-1}) of the indicated mAb treatment by intraperitoneal injection. Tissues were collected at six days after infection. For all panels, infectious virus in lung homogenates was determined by plaque assay using Vero-hACE2-TMPRSS2 cells (line indicates median; in order from left to right $n = 5, 5, 5, 6, 6$ and 6 (**a**); $n = 6, 6, 6, 6, 6$ and 6 (**b**–**h**) mice per group, one-way ANOVA with Dunnett's test with comparison to control mAb: ns, not significant, $^{****}P < 0.0001$; $^{**}P = 0.0012$, $^{***}P = 0.0003$ (**c**); $^{**}P = 0.0048$, $^{***}P = 0.0005$ (**e**); $^{**}P = 0.0031$, 0.0019 and 0.0020 (**f**, from left to right)). Dotted lines indicate the limit of detection of the assay.

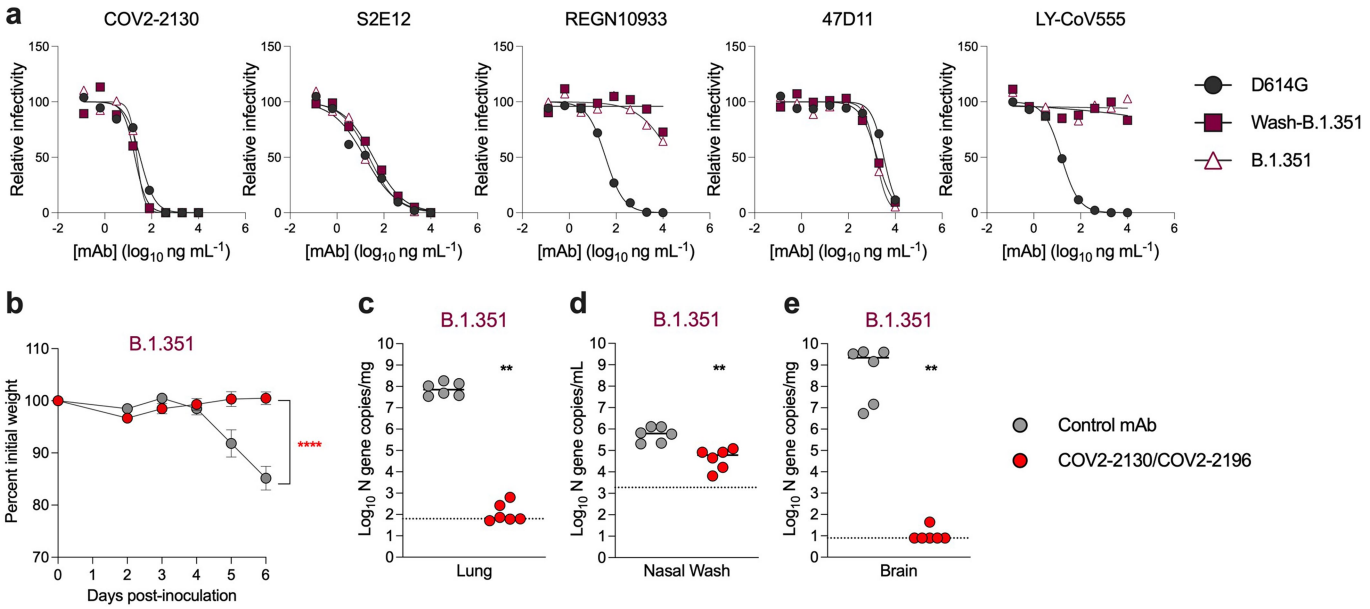

Extended Data Fig. 4 | Antibody neutralization and protection against a natural B.1.351 isolate. a, Selected anti-SARS-CoV-2 mAbs (one from each cocktail) were tested for neutralization of infection by WA1/2020 D614G, Wash-B.1.351 or B.1.351 on Vero-TMPRSS2 cells using an focus reduction neutralization test (FRNT). One representative experiment of two performed in duplicate is shown. **b**–**e**, Eight-to-ten-week-old female K18-hACE2 transgenic mice received 40 µg (about 2 mg kg^{-1}) of control mAb or COV2-2130/COV2-2196 by intraperitoneal injection one day before intranasal inoculation with 10^3 FFU of B.1.351. **b**, Weight change following infection (mean ± s.e.m.; $n = 6$ mice per group, two experiments; one-way ANOVA with Dunnett's test of area under the curve: ns, not significant, $^{****}P < 0.0001$). Viral RNA levels in the lung (**c**), nasal wash (**d**) and brain (**e**) (line indicates median; $n = 6$ mice per group, two experiments; Mann–Whitney test: $^{**}P = 0.002$ (**c**–**e**)). Dotted line indicates the limit of detection of the assay.

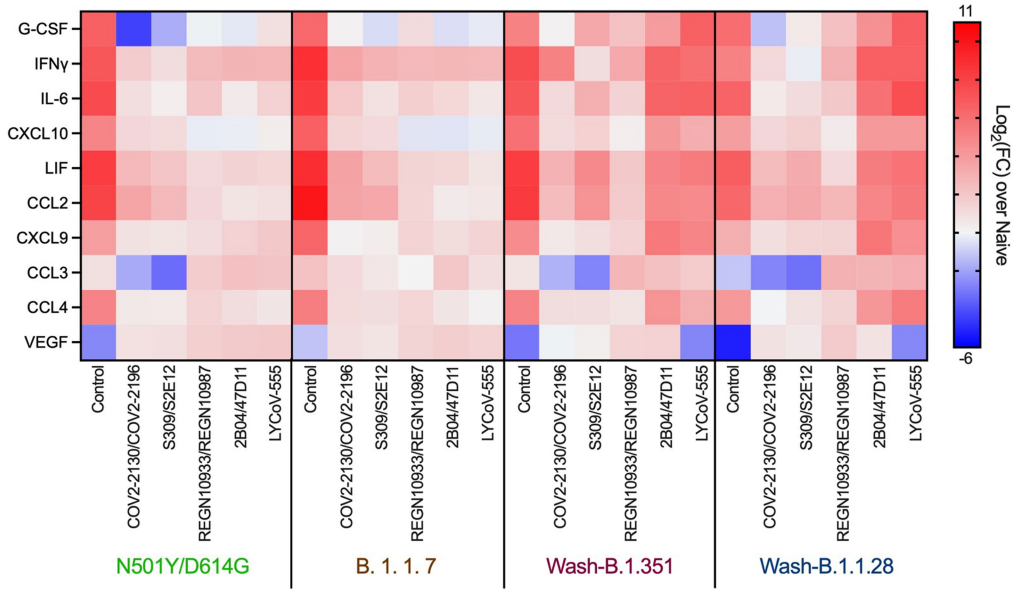

Extended Data Fig. 5 | Antibody-mediated protection against SARS-CoV-2-induced inflammation. Eight-to-ten-week-old female and male K18-hACE2 transgenic mice received 40 µg (about 2 mg kg^{-1}) of the indicated mAb treatment by intraperitoneal injection one day before intranasal inoculation with 10^3 FFU of the indicated SARS-CoV-2 strain. Heat map of cytokine and chemokine protein expression levels in lung homogenates collected at six days after infection from the indicated groups. Data are presented as log_2-transformed fold change over naive mice. Blue, reduction; red, increase.

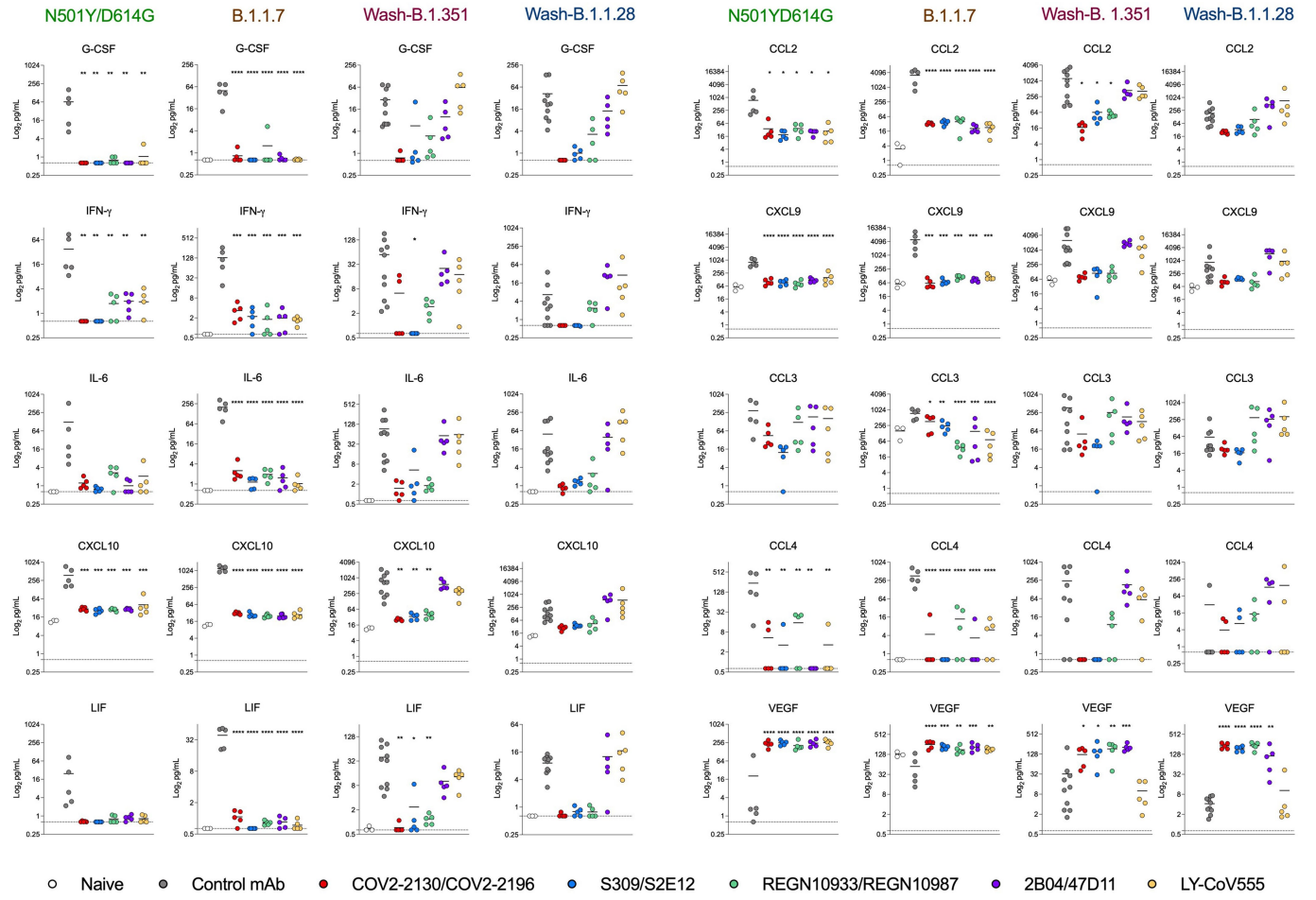

Extended Data Fig. 6 | Cytokine and chemokine induction following SARS-CoV-2 infection. Individual plots for cytokine and chemokine protein levels in the lungs of antibody-treated K18-hACE2 transgenic mice at 6 days after infection with the indicated SARS-CoV-2 strain (line indicates mean; $n = 3$ naive, $n = 5$ for all other groups of B.1.1.7- and N501Y-infected mice; $n = 3$ naive, 10 control, 5 for all other groups of Wash-B.1.351- and Wash-B.1.1.28-infected mice; one-way ANOVA with Dunnett's test with comparison to control mAb: ns, not significant, $^{****}P < 0.0001$; all other P values are listed in Supplementary Table 5). Select cytokines and chemokines were used to generate the heat map in Extended Data Fig. 5.

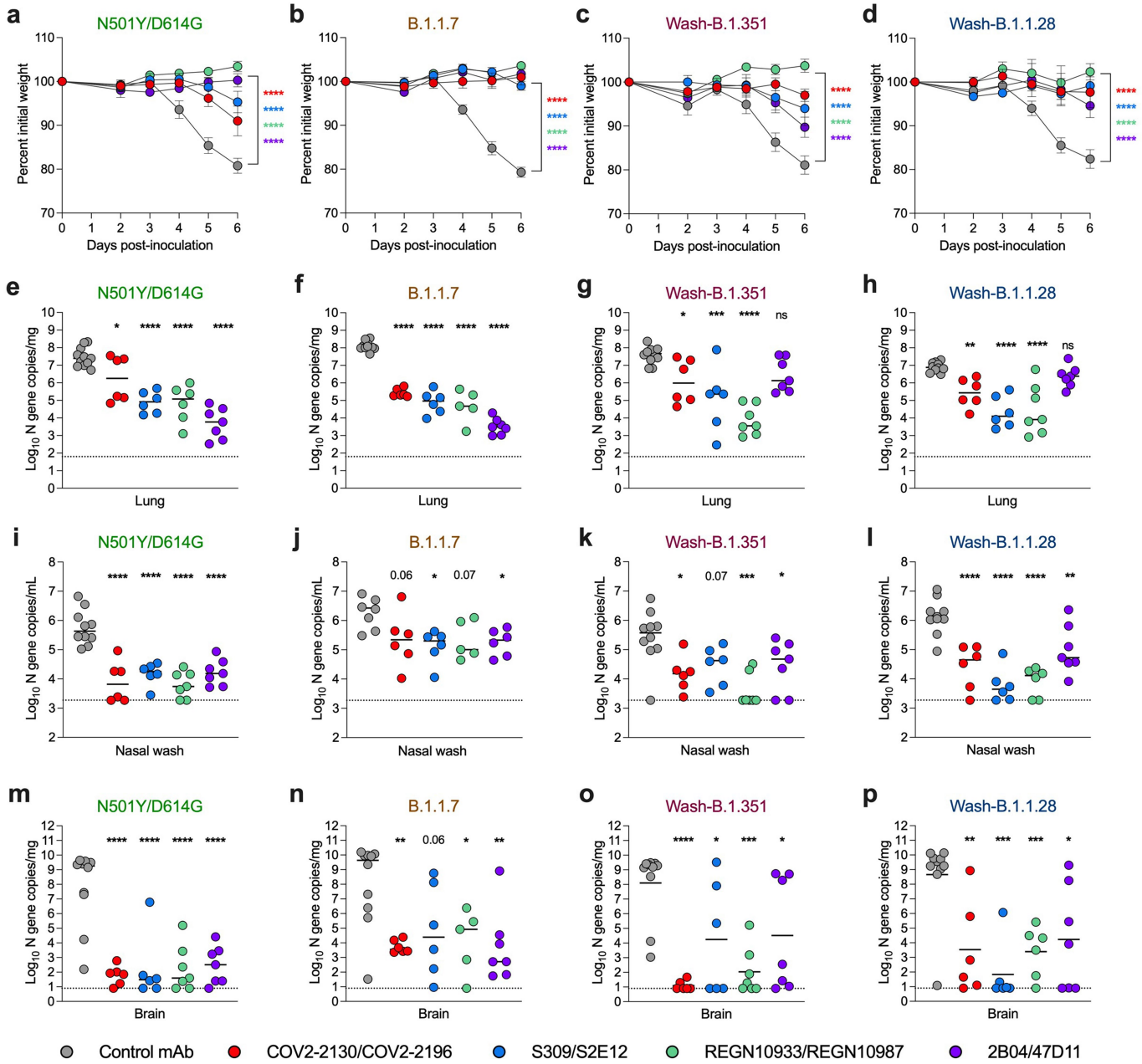

Extended Data Fig. 7 | Low-dose antibody prophylaxis against SARS-CoV-2 variants in K18-hACE2 mice. a–**p**, Eight-to-ten-week-old female and male K18-hACE2 transgenic mice received 4 μg (about 0.2 mg kg^{-1}) of the indicated mAb treatment by intraperitoneal injection one day before intranasal inoculation with 10^3 FFU of the indicated SARS-CoV-2 strain. Tissues were collected at six days after infection. **a**–**d**, Weight change following infection with SARS-CoV-2 (mean ± s.e.m.; in order from left to right $n = 11, 6, 6$ and 7, 7 (**a**); $n = 10, 6, 6, 5$ and 7 (**b**); $n = 10, 6, 6, 7$ and 7 (**c**, **d**) mice per group, two experiments; one-way ANOVA with Dunnett's test of area under the curve with comparison to control mAb: ****$P < 0.0001$). Viral RNA levels in the lung (**e**–**h**), nasal wash (**i**–**l**) or brain (**m**–**p**) were measured (line indicates median; in order from left to right $n = 11, 6, 6, 6$ and 7 (**e**); $n = 10, 6, 6, 5$ and 7 (**f**, **n**); $n = 10, 6, 6, 7$ and 7 (**g**–**i**, **k**, **m**, **o**); $n = 8, 6, 6, 5$ and 6 (**j**); $n = 10, 6, 6, 6$ and 7 (**l**, **p**) mice per group, two experiments; one-way ANOVA with Dunnett's test with comparison to isotype control mAb: ns, not significant, ****$P < 0.0001$); *$P = 0.034$ (**e**); *$P = 0.0422$, ***$P = 0.0004$ (**g**); **$P = 0.0080$ (**h**); *$P = 0.0209$ (left), 0.0365 (right) (**j**); *$P = 0.0124$ (left), 0.0497 (right), ***$P = 0.0001$ (**k**); **$P = 0.0069$ (**l**); **$P = 0.0087$ (left), 0.0061 (right), *$P = 0.0264$ (**n**); *$P = 0.0378$ (left), 0.0446 (right), ***$P = 0.0004$ (**o**); **$P = 0.0045$ (left), 0.0035 (right), ***$P = 0.0002$, * = 0.0107 (**p**)). Dotted line indicates the limit of detection of the assay.

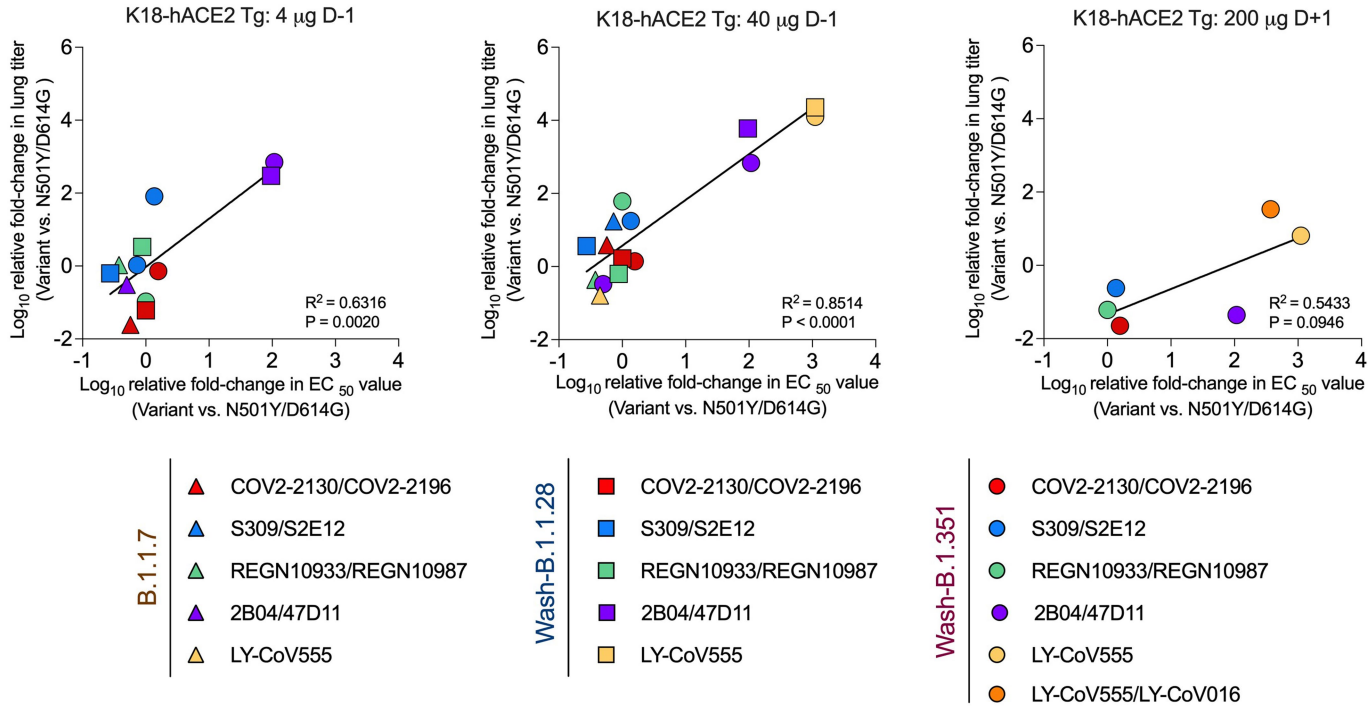

Extended Data Fig. 8 | In vivo correlation of antibody-mediated protection against SARS-CoV-2. For each panel, the fold change in the EC_{50} values of the indicated mAb or mAb cocktails between the N501Y/D614G strain and one or more variants of concern (B.1.1.7, Wash-B.1.351 or Wash-B.1.1.28) were plotted on the *x* axis. Next, the fold change in lung viral RNA titre corresponding to the indicated treatment group (top labels) between the N501Y/D614G strain and one or more variants of concern (B.1.1.7, Wash-B.1.351 or Wash-B.1.1.28) were plotted on the *y* axis. Best-fit lines were calculated using a simple linear regression. Two-tailed Pearson correlation was used to calculate R^2 and *P* values indicated within each panel.

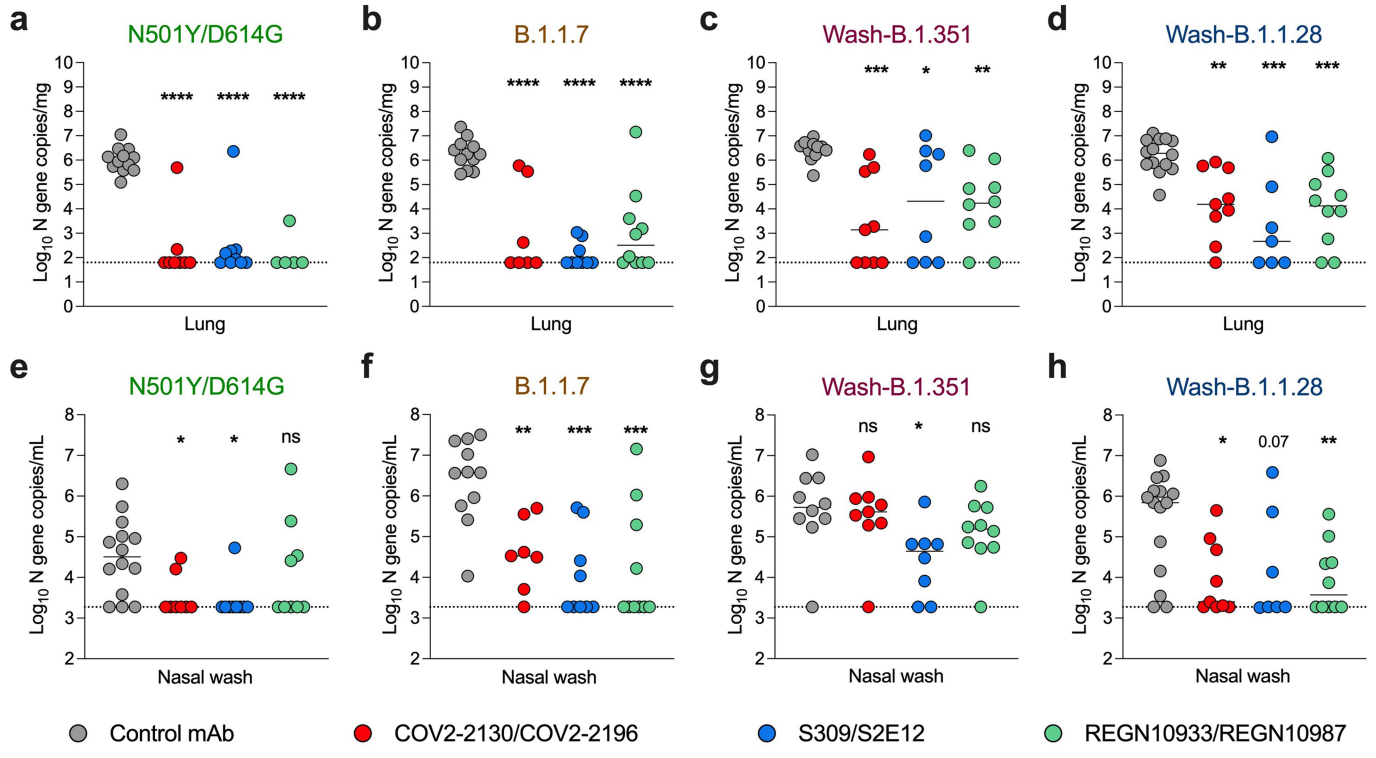

Extended Data Fig. 9 | Antibody-mediated protection against SARS-CoV-2 variants in 129S2 mice. a–h, Six-to-seven-week-old female and male immunocompetent 129S2 mice received 40 μg (about 2 mg kg^{-1}) of the indicated mAb treatment by intraperitoneal injection one day before intranasal inoculation with 10^3 FFU of WA1/2020 N501Y/D614G, Wash-B.1.351 or Wash-B.1.1.28 or 10^5 FFU of B.1.1.7. Tissues were collected at three days after infection. Viral RNA levels in the lung (**a**–**d**) or nasal washes (**e**–**h**) were determined (line indicates median; in order from left to right n = 12, 8, 6 and 5 (**a**); n = 12, 7, 9 and 10 (**b**); n = 11, 9, 8 and 10 (**c**); n = 14, 9, 6 and 5 (**d**); n = 14, 5, 9 and 9 (**e**); n = 11, 7, 9 and 10 (**f**); n = 10, 9, 8 and 10 (**g**); n = 15, 9, 7 and 10 (**h**) mice per group, pooled from two to three experiments; one-way ANOVA with Dunnett's test with comparison to control mAb: ns, not significant, ***P < 0.001; ***P = 0.0009, *P = 0.0176, **P = 0.0077 (**c**); **P = 0.0042, ***P = 0.0001 (left), 0.0010 (right) (**d**); *P = 0.0467 (left), 0.0188 (right) (**e**); **P = 0.0059, ***P = 0.0002 (left), 0.0004 (right) (**f**); *P = 0.0184 (**g**), *P = 0.0129, **P = 0.0090 (**h**)). Dotted line indicates the limit of detection of the assay.

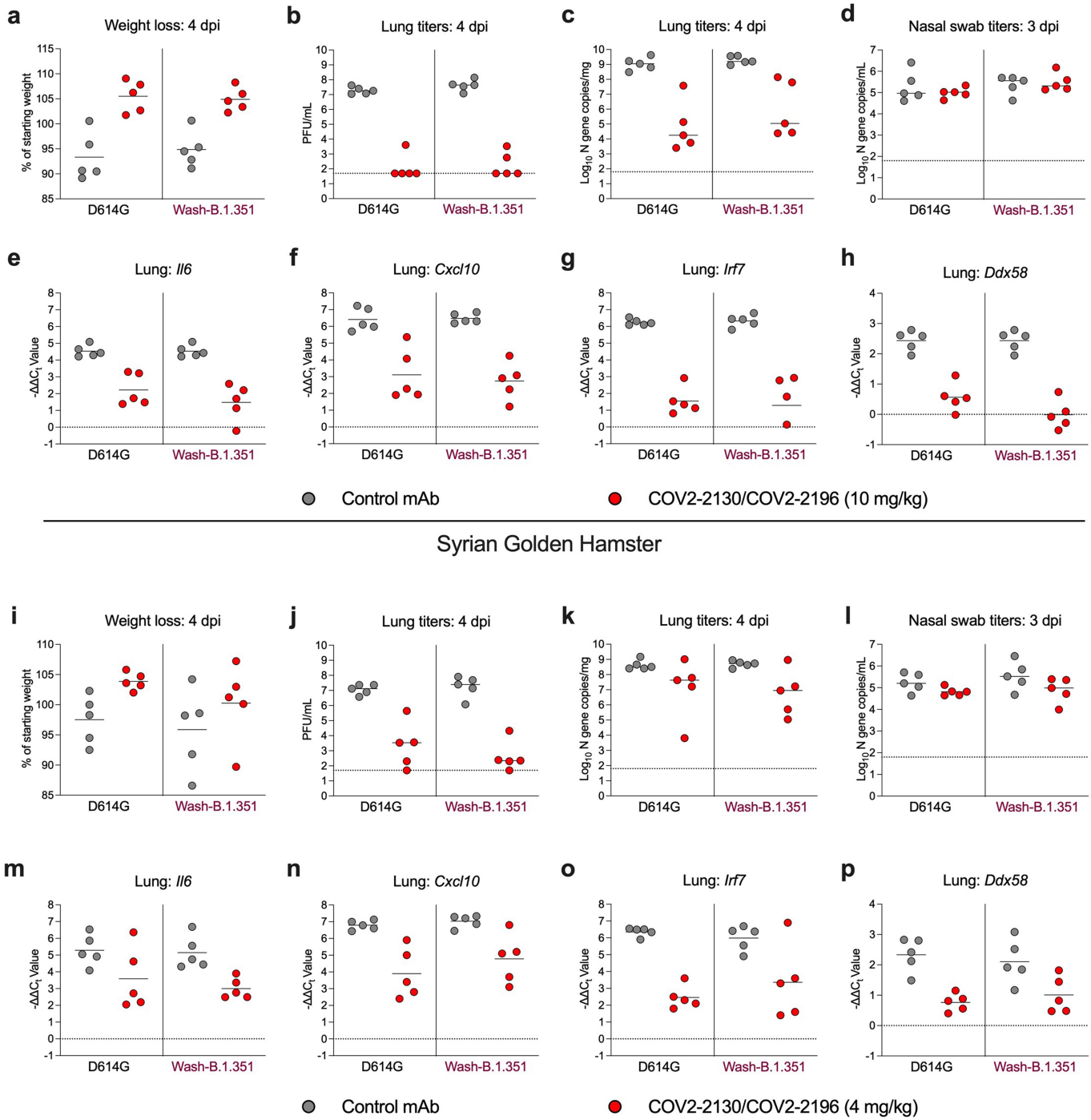

Extended Data Fig. 10 | COV2-2130/COV2-2196 antibody cocktail protects hamsters against historical and variant SARS-CoV-2 strains. Six-week-old male Syrian golden hamsters received a single 800 µg (about 10 mg kg^{-1}) (**a**–**h**) or 320 µg (about 4 mg kg^{-1}) dose (**i**–**p**) of COV2-2130/COV2196 mAb cocktail or control mAb by intraperitoneal injection one day before intranasal inoculation with 5×10^5 FFU of WA1/2020 D614G or Wash-B.1.351 viruses. Nasal swabs and lung tissues were collected at three and four days after infection, respectively. **a**, **i**, Weight change following infection with SARS-CoV-2 (line indicates mean; $n = 5$ hamsters per group, one experiment). Infectious virus in the lung (**b**, **j**) or viral RNA levels in the lung (**c**, **k**) and nasal swabs (**d**, **l**) were determined (line indicates median; $n = 5$ hamsters per group, one experiment). Dotted line indicates the limit of detection of the assay. **e**–**h**, **m**–**p**, Cytokine and inflammatory gene expression in lung homogenates collected at 6 days after infection from indicated groups (line indicates mean; $n = 5$ hamsters per group). Values were calculated using the $\Delta\Delta C_t$ method compared to a naive control group. Because data were obtained from a single experiment (even with multiple hamsters), statistical analysis was not performed.

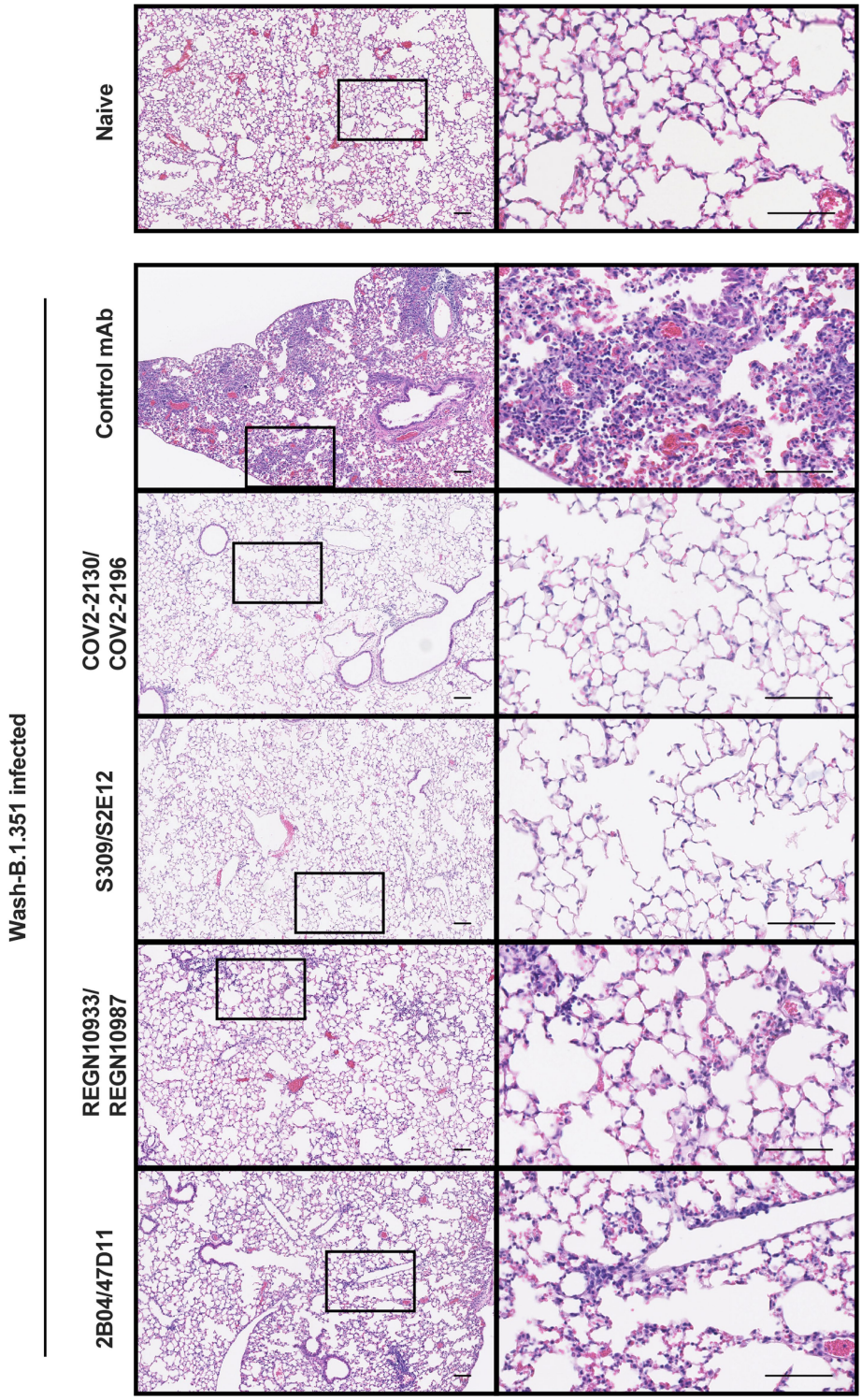

Extended Data Fig. 11 | Antibody protection against SARS-CoV-2 induced lung pathology. Eight-to-ten-week-old female K18-hACE2 transgenic mice received 200 µg (about 10 mg kg^{-1}) of the indicated mAb treatment or isotype control by intraperitoneal injection one day after intranasal inoculation with 10^3 FFU of Wash-B.1.351 SARS-CoV-2. At six days after infection, mice were killed and lungs fixed for sectioning before staining with haematoxylin and eosin. A lung section from a naive, uninfected mouse is shown (top panels) as a reference control. Images show low (left panels for each treatment) and high (right panels for each treatment; boxed region from left) resolution. Scale bars, 100 µm. Representative images from $n = 3$ mice per group.

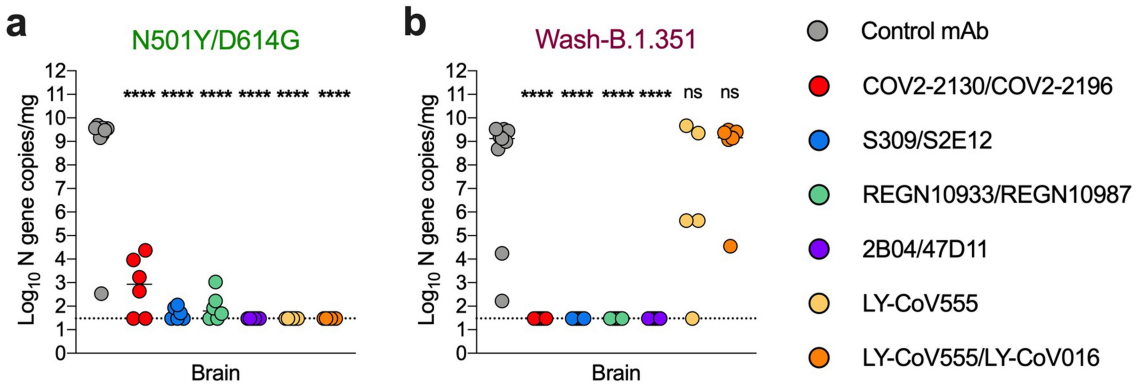

Extended Data Fig. 12 | Post-exposure antibody therapy against SARS-CoV-2 variants in K18-hACE2 mice. a, **b**, Eight-to-ten-week-old female and male K18-hACE2 transgenic mice were administered 10^3 FFU of the indicated SARS-CoV-2 strain by intranasal inoculation. One day later, mice received 200 µg (about 10 mg kg^{-1}) of the indicated mAb treatment by intraperitoneal injection. Brain tissues were collected at six days after infection. Viral RNA levels are shown (**a**, **b**) (line indicates median; in order from left to right $n = 9, 6, 6, 6, 6, 6$ and 6 (**a**); $n = 7, 6, 6, 6, 6, 5$ and 7 (**b**) mice per group, two experiments; one-way ANOVA with Dunnett's test with comparison to control mAb: ns, not significant, $^{****}P < 0.0001$). Dotted line indicates the limit of detection of the assay.

a

Neutralization on Vero-TMPRSS2 cells	SARS-CoV-2 Viruses								
mAbs EC_{50} (ng/mL)	D614G	N501Y/D614G	B.1.1.7	Wash-B.1.351	Wash-B.1.1.28	B.1.429	B.1.617.1	B.1.526 (S477N)	B.1.526 (E484K)
LY-CoV016	52	290	169	>10,000	>10,000	38	20	9	99
LY-CoV555/LY-CoV016	9	27	11	>10,000	>10,000	63	65	3	261

b

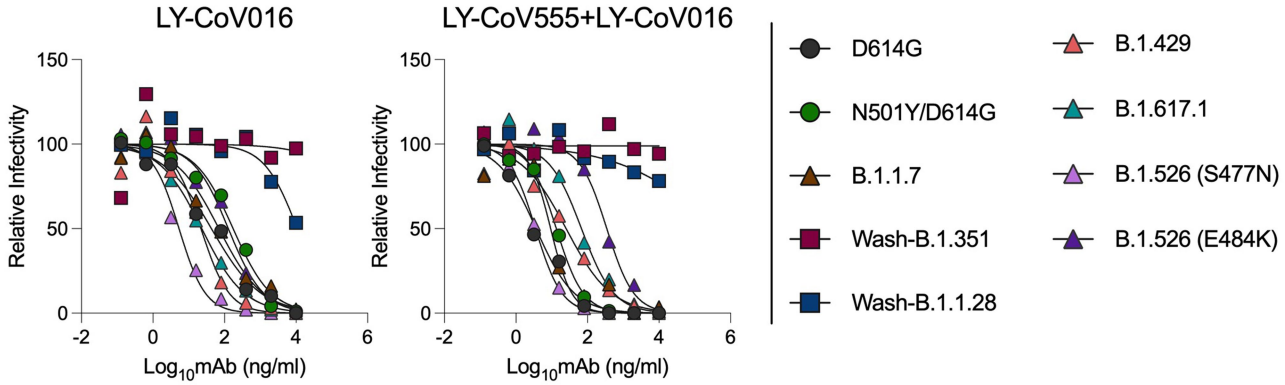

Extended Data Fig. 13 | Neutralization curves with mAb LY-CoV016 as monotherapy and combination with variant SARS-CoV-2 strains. **a**, **b**, Anti-SARS-CoV-2 human mAb LY-CoV016 and combination LY-CoV555/LY-CoV016 (parental mAbs of bamlanivimab and etesevimab, respectively) were tested for inhibition of infection of the indicated SARS-CoV-2 viruses using a FRNT. EC_{50} values (ng ml^{-1}) (**a**) and one representative experiment of two performed in duplicate is shown (**b**).

nature research

Corresponding author(s): Michael Diamomd

Last updated by author(s): 06/04/2021

Reporting Summary

Nature Research wishes to improve the reproducibility of the work that we publish. This form provides structure for consistency and transparency in reporting. For further information on Nature Research policies, see our Editorial Policies and the Editorial Policy Checklist.

Statistics

For all statistical analyses, confirm that the following items are present in the figure legend, table legend, main text, or Methods section.

n/a	Confirmed	
☐	☒	The exact sample size (*n*) for each experimental group/condition, given as a discrete number and unit of measurement
☐	☒	A statement on whether measurements were taken from distinct samples or whether the same sample was measured repeatedly
☐	☒	The statistical test(s) used AND whether they are one- or two-sided *Only common tests should be described solely by name; describe more complex techniques in the Methods section.*
☒	☐	A description of all covariates tested
☒	☐	A description of any assumptions or corrections, such as tests of normality and adjustment for multiple comparisons
☐	☒	A full description of the statistical parameters including central tendency (e.g. means) or other basic estimates (e.g. regression coefficient) AND variation (e.g. standard deviation) or associated estimates of uncertainty (e.g. confidence intervals)
☐	☒	For null hypothesis testing, the test statistic (e.g. *F*, *t*, *r*) with confidence intervals, effect sizes, degrees of freedom and *P* value noted *Give P values as exact values whenever suitable.*
☒	☐	For Bayesian analysis, information on the choice of priors and Markov chain Monte Carlo settings
☒	☐	For hierarchical and complex designs, identification of the appropriate level for tests and full reporting of outcomes
☒	☐	Estimates of effect sizes (e.g. Cohen's *d*, Pearson's *r*), indicating how they were calculated

Our web collection on statistics for biologists contains articles on many of the points above.

Software and code

Policy information about availability of computer code

Data collection	No software was used in this study to collect data
Data analysis	Prism 8.0 was used to perform all statistical analysis. BWA4 v0.7.17-r1188 (http://bio-bwa.sourceforge.net). DeepVariant4 v1.1.0 (https://github.com/google/deepvariant) was used to call variants with an allele frequency >= 50%. Variants were annotated using SNPEff4 5.0c (https://sourceforge.net/projects/snpeff/). Structural figures were generated using UCSF ChimeraX (https://www.cgl.ucsf.edu/chimerax/)

For manuscripts utilizing custom algorithms or software that are central to the research but not yet described in published literature, software must be made available to editors and reviewers. We strongly encourage code deposition in a community repository (e.g. GitHub). See the Nature Research guidelines for submitting code & software for further information.

Data

Policy information about availability of data

All manuscripts must include a data availability statement. This statement should provide the following information, where applicable:

- Accession codes, unique identifiers, or web links for publicly available datasets
- A list of figures that have associated raw data
- A description of any restrictions on data availability

The authors declare that all data supporting the findings of this study are available within the paper and its Supplementary information. All data supporting the findings of this study are available from the corresponding author upon request.

Field-specific reporting

Please select the one below that is the best fit for your research. If you are not sure, read the appropriate sections before making your selection.

☒ Life sciences ☐ Behavioural & social sciences ☐ Ecological, evolutionary & environmental sciences

For a reference copy of the document with all sections, see nature.com/documents/nr-reporting-summary-flat.pdf

Life sciences study design

All studies must disclose on these points even when the disclosure is negative.

Sample size	No sample sizes were chosen a priori. All experiments with statistical analysis were repeated at least two independent times, each with multiple technical replicates. Experimental size of cohorts was determined based on prior experience performing studies in mice.
Data exclusions	No data was excluded.
Replication	All experiments had multiple biological and/or technical replicates and are indicated the Figure legends.
Randomization	For animal studies, mice were randomly assigned to treatment groups in an age and sex-matched distribution.
Blinding	No blinding was performed although several key studies were performed independently by different members of the laboratory.

Reporting for specific materials, systems and methods

We require information from authors about some types of materials, experimental systems and methods used in many studies. Here, indicate whether each material, system or method listed is relevant to your study. If you are not sure if a list item applies to your research, read the appropriate section before selecting a response.

Materials & experimental systems

n/a	Involved in the study
☐	☒ Antibodies
☐	☒ Eukaryotic cell lines
☒	☐ Palaeontology and archaeology
☐	☒ Animals and other organisms
☒	☐ Human research participants
☒	☐ Clinical data
☒	☐ Dual use research of concern

Methods

n/a	Involved in the study
☒	☐ ChIP-seq
☒	☐ Flow cytometry
☒	☐ MRI-based neuroimaging

Antibodies

Antibodies used	MAbs: hWNV-E16, COV2-2196, COV2-2130, S309, S2E12, 2B04, 47D11, REGN10933, REGN10987, CB6 [LY-CoV016], and LY-CoV555; Also: pool of SARS2-2, SARS2-11, SARS2-16, SARS2-31, SARS2-38, SARS2-57, and SARS2-71 for focus assays; None of these mAbs are available commercially and were either generated in the Diamond laboratory (SARS2-2, SARS2-11, SARS2-16, SARS2-31, SARS2-38, SARS2-57, and SARS2-71), Crowe laboratory (COV2-2130 and COV2-2196), Vir (S309 and S2E12), Abbvie (2B04 and 47D11) or synthesized from published sequences. The antibodies were used at a range of concentrations as indicated in the Figures. HRP-conjugated goat anti-mouse IgG (Sigma 12-349, 1/1000)
Validation	All primary mAbs were validated using purified SARS-CoV-2 RBD or S proteins using ELISA or BLI assays.

Eukaryotic cell lines

Policy information about cell lines

Cell line source(s)	Vero-TMPRSS2, Diamond laboratory; Vero-hACE2-TMPRSS2, Graham laboratory, VRC/NIH;
Authentication	These were obtained from academic laboratories and grew and performed as expected. Cells expressing TMPRSS2 and hACE2 were validated using monoclonal antibodies and flow cytometry.
Mycoplasma contamination	All cell lines are routinely tested each month and were negative for mycoplasma.
Commonly misidentified lines (See ICLAC register)	This study did not involve any commonly misidentified cell lines.

Animals and other organisms

Policy information about studies involving animals; ARRIVE guidelines recommended for reporting animal research

Laboratory animals	K18-hACE2 transgenic mice (both sexes, 8-10-week-old), 129S2 mice (both sexes, 6-7 week-old); Syrian Golden hamsters (male, 6 month-old). Mice were housed in groups of 4 to 5; Hamsters were housed alone. Photoperiod = 12 hr on:12 hr off dark/light cycle. Ambient animal room temperature is 70° F, controlled within ±2° and room humidity is 50%, controlled within ±5%.
Wild animals	No wild animals were used in this study.
Field-collected samples	No field collected samples were used in this study.
Ethics oversight	All experiments were conducted with approval of the Institutional Animal Care and Use Committee at the Washington University School of Medicine (Assurance number A3381-01)

Note that full information on the approval of the study protocol must also be provided in the manuscript.